NATIONAL HURRICANE RESEARCH PROJECT

REPORT NO. 49

Some Properties of Hurricane Wind Fields as Deduced from Trajectories

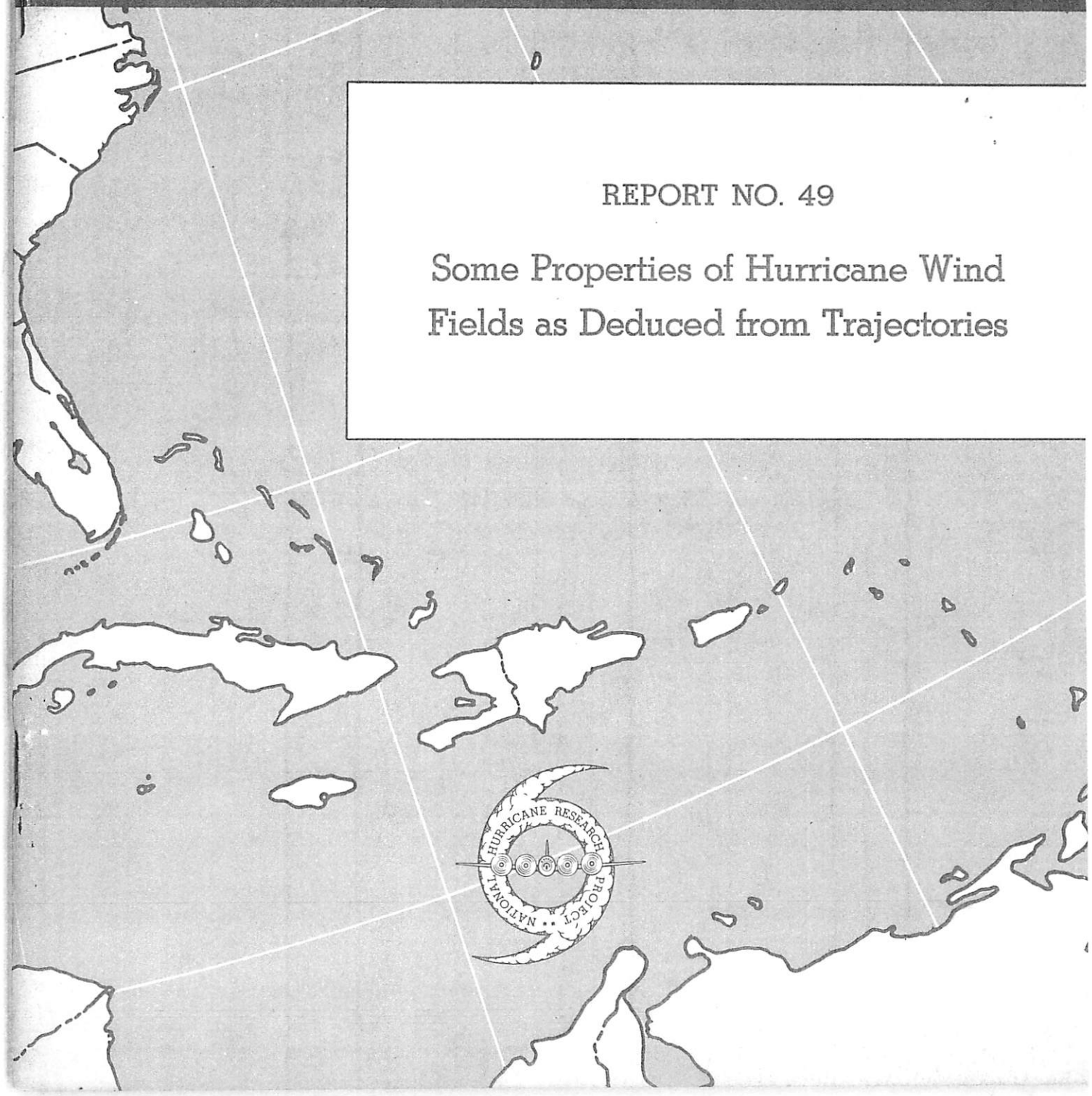

U. S. DEPARTMENT OF COMMERCE
Luther H. Hodges, Secretary
WEATHER BUREAU
F. W. Reichelderfer, Chief

NATIONAL HURRICANE RESEARCH PROJECT

REPORT NO. 49

Some Properties of Hurricane Wind Fields as Deduced from Trajectories

by
Vance A. Myers and William Malkin
Hydrometeorological Section, Hydrologic Services Division,
U. S. Weather Bureau, Washington, D. C.

Washington, D. C.
November 1961

NATIONAL HURRICANE RESEARCH PROJECT REPORTS

Reports oy Weather Bureau units, contractors, and cooperators working on the hurricane problem are preprinted in this series to facilitate immediate distribution of the information among the workers and other interested units. As this limited reproduction and distribution in this form do not constitute formal scientific publication, reference to a paper in the series should identify it as a preprinted report.

No. 1. Objectives and basic design of the NHRP. March 1956.
No. 2. Numerical weather prediction of hurricane motion. July 1956.
Supplement: Error analysis of prognostic 500-mb. maps made for numerical weather prediction of hurricane motion. March 1957.
No. 3. Rainfall associated with hurricanes. July 1956.
No. 4. Some problems involved in the study of storm surges. December 1956.
No. 5. Survey of meteorological factors pertinent to reduction of loss of life and property in hurricane situations. March 1957.
No. 6. A mean atmosphere for the West Indies area. May 1957.
No. 7. An index of tide gages and tide gage records for the Atlantic and Gulf coasts of the United States. May 1957.
No. 8. Part I. Hurricanes and the sea surface temperature field. Part II. The exchange of energy between the sea and the atmosphere in relation to hurricane behavior. June 1957.
No. 9. Seasonal variations in the frequency of North Atlantic tropical cyclones related to the general circulation. July 1957.
No. 10. Estimating central pressure of tropical cyclones from aircraft data. August 1957.
No. 11. Instrumentation of National Hurricane Research Project aircraft. August 1957.
No. 12. Studies of hurricane spiral bands as observed on radar. September 1957.
No. 13. Mean soundings for the hurricane eye. September 1957.
No. 14. On the maximum intensity of hurricanes. December 1957.
No. 15. The three-dimensional wind structure around a tropical cyclone. January 1958.
No. 16. Modification of hurricanes through cloud seeding. May 1958.
No. 17. Analysis of tropical storm Frieda 1957. A preliminary report. June 1958.
No. 18. The use of mean layer winds as a hurricane steering mechanism. June 1958.
No. 19. Further examination of the balance of angular momentum in the mature hurricane. July 1958.
No. 20. On the energetics of the mature hurricane and other rotating wind systems. July 1958.
No. 21. Formation of tropical storms related to anomalies of the long-period mean circulation. September 1958.
No. 22. On production of kinetic energy from condensation heating. October 1958.
No. 23. Hurricane Audrey storm tide. October 1958.
No. 24. Details of circulation in the high energy core of hurricane Carrie. November 1958.
No. 25. Distribution of surface friction in hurricanes. November 1958.
No. 26. A note on the origin of hurricane radar spiral bands and the echoes which form them. February 1959.
No. 27. Proceedings of the Board of Review and Conference on Research Progress. March 1959.
No. 28. A model hurricane plan for a coastal community. March 1959.
No. 29. Exchange of heat, moisture, and momentum between hurricane Ella (1958) and its environment. April 1959.
No. 30. Mean soundings for the Gulf of Mexico area. April 1959.
No. 31. On the dynamics and energy transformations in steady-state hurricanes. August 1959.
No. 32. An interim hurricane storm surge forecasting guide. August 1959.
No. 33. Meteorological considerations pertinent to standard project hurricane, Atlantic and Gulf coasts of the United States. November 1959.
No. 34. Filling and intensity changes in hurricanes over land. November 1959.
No. 35. Wind and pressure fields in the stratosphere over the West Indies region in August 1958. December 1959.
No. 36. Climatological aspects of intensity of typhoons. February 1960.
No. 37. Unrest in the upper stratosphere over the Caribbean Sea during January 1960. April 1960.
No. 38. On quantitative precipitation forecasting. August 1960.
No. 39. Surface winds near the center of hurricanes (and other cyclones). September 1960.
No. 40. On initiation of tropical depressions and convection in a conditionally unstable atmosphere. October 1960.
No. 41. On the heat balance of the troposphere and water body of the Caribbean Sea. December 1960.
No. 42. Climatology of 24-hour North Atlantic tropical cyclone movements. January 1961.
No. 43. Prediction of movements and surface pressures of typhoon centers in the Far East by statistical methods. May 1961.
No. 44. Marked changes in the characteristics of the eye of intense typhoons between the deepening and filling states. May 1961.
No. 45. The occurrence of anomalous winds and their significance. June 1961.
No. 46. Some aspects of hurricane Daisy, 1958. July 1961.
No. 47. Concerning the mechanics and thermodynamics of the inflow layer of the mature hurricane. September 1961.
No. 48. On the structure of hurricane Daisy (1958). October 1961.

USCOMM-WB-DC

CONTENTS

LIST OF SYMBOLS

A = area(s) of small polygon(s), computed at successive times, used in the computation of horizontal divergence and convergence

b = subscript indicating item pertains to the equilibrium wind value

e = the base of natural logarithms

f = Coriolis parameter, $2\omega\sin\psi$

F = horizontal frictional force per unit mass

F_t = the component of F tangent to the trajectory, positive opposite the wind

F_n = the component of F normal to the trajectory, positive in the direction of positive n

$\vec{k}$ = conventional vertical unit vector

K_t = an empirically determined constant relating F_t to the square of the velocity

K_n = an empirically determined constant relating F_n to the square of the velocity

m = a constant

n = distance normal to a trajectory, positive to the right of s

p = pressure

p_o = central pressure

p_n = pressure at the periphery of a storm

r = distance along a radius of the hurricane or radius vector of a point from the hurricane center, positive outward from the center

r_T = radius of curvature of a trajectory

R = radius of maximum winds

s = distance along a trajectory

$\vec{V}, V$ = wind velocity, wind speed

V_g = geostrophic wind

V_H = velocity of hurricane

Z = vertical distance

α = wind direction angle, clockwise from direction of storm motion

β = deflection angle, positive when inward toward lower pressure

θ = azimuth angle, positive when measured clockwise from the direction of motion of the storm

ρ = density of air

τ = horizontal shearing stress

$\vec{\nabla}_2$ = the two-dimensional (horizontal) operator,

$$\frac{\partial}{\partial x} + \frac{\partial}{\partial y}$$

$\overline{}$ = bar indicating average value of a quantity

SOME PROPERTIES OF HURRICANE WIND FIELDS AS DEDUCED FROM TRAJECTORIES

Vance A. Myers and William Malkin
Hydrometeorological Section, Hydrologic Services Division
U. S. Weather Bureau, Washington, D. C.

[Manuscript received June 23, 1961]

ABSTRACT

Surface wind fields for hurricanes are simulated by a trajectory technique. Both normal and tangential components of friction are considered. The technique applies to a moving as well as a stationary storm and only the pressure profile and frictional coefficients need be specified. The trajectory technique is applied to test several theoretical suppositions, some of which are developed from equations of motion. Among the aspects considered are (a) causes and character of the asymmetry of surface wind fields, and (b) wind field modifications due to motion of the hurricane, variation in pressure gradient, and variation in frictional coefficients.

An "equilibrium wind" concept for flow with friction is suggested as a logical counterpart to the gradient wind for flow with friction neglected.

1. INTRODUCTION

There are many problems that require an adequate description of the surface wind field in hurricanes. Such information is useful for forecasting and navigating, is required in estimating the wind field over areas with no observations, and is fundamental to an understanding of the formation, life history and structure of tropical storms. The particular problem that prompted this study was a requirement for patterns of surface wind speeds and directions in hurricanes that might at some future time affect coastal regions. These wind fields are used to estimate tides and waves that the storms might produce. The height and duration of the tides and waves are in turn considered in the design of hurricane protective works.

When the essential morphological characteristics of a hurricane, such as the pressure profile and the distribution of radar echoes, in addition to information concerning the storm's movement, are known the problem of describing the surface wind field remains. To the present time, there have not been sufficient knowledge and data on the distribution of wind speeds and directions in hurricanes to develop an adequate quantitative model of what to expect in severe hurricanes of the future. Further, for the purpose of surge

computations, a hurricane model yielding average wind speeds over a period of several hours is desirable. Even if a dense network of individual observations were made available at some future time, an additional requirement would be for observations not influenced by the short-period wind variations known to exist in hurricanes. The model would serve to define a rational average velocity field, both in space and time.

A needed approach, therefore, seemed to be the development of a dynamic model of the surface wind field of a hurricane which could lead to more comprehensive analysis and interpretation of such data as are available and provide representative wind values for all regions of the storm.

The objectives of this study were, specifically:

(1) To obtain characteristics of the horizontal surface wind fields in a hurricane by deductions from the governing equations of motion;

(2) To verify these deductions and draw additional conclusions by constructing dynamic trajectories in a model hurricane; and

(3) To formulate from these characteristics and conclusions a substitute for the patently untenable hypothesis that the physical cause of the asymmetry of the hurricane surface wind field is to be found in the vector addition of distinctive components of rotation and translation.

The first objective is treated in sections 3 and 4. The second objective is introduced in section 2, and is developed in sections 5 through 9. The final objective is covered in section 11. Section 10 contains material of a preliminary nature on the energy source, which is in addition to the basic objectives of the study.

2. TRAJECTORIES IN A MODEL HURRICANE

Radial profiles and horizontal maps of the wind in the friction layer of a model hurricane were obtained by graphically constructing dynamic trajectories through a model pressure field, starting with initial wind values at an outer boundary. The trajectories were constructed by a stepwise, so-called "arc-strike" technique, developed and explained by Goodyear /3/. Modifications of Goodyear's method were introduced in order to incorporate the accelerations due to both normal and tangential friction*. The outer boundary was at a radius of 120 miles from the hurricane center; thus the study was concentrated on the more vigorous part of the storm.

*Throughout this paper, "friction" and "frictional acceleration" are synonymous terms referring to the frictional force per unit mass derived from the variation of horizontal shearing stress with height. This term, $\frac{1}{\rho}\frac{\partial \tau}{\partial z}$, has the dimensions of acceleration. The "friction coefficient" is the proportionality factor, having dimensions of length^{-1}, which factor when multiplied by the square of the wind speed, gives the frictional acceleration.

Earlier attempts by collaborators of the authors to simulate airflow in a hurricane without incorporating the effects of friction, and by considering tangential friction only, gave unsatisfactory results. Without friction a trajectory with initial incurvature resembles a segment of the orbit of an asteroid. The trajectory swings in to a point of tangency with a circle about the center and then swings out again on the opposite side of the storm. With tangential friction only, the opposite extreme was encountered. Trajectories dived toward the storm center at excessive crossing angles. Haurwitz /6/ has referred to the use of tangential friction only (in a sea breeze) as "admittedly crude." Other studies have reported normal components of friction (Godske, et al. /2/, Hubert /7/, Myers /15/) of about the same order of magnitude as the tangential component.

Of the frictional coefficients available from earlier studies those determined by Myers /15/ in the hurricane of August 26-27, 1949 over Lake Okeechobee, Florida, were considered the most nearly applicable to hurricane wind flow over a water surface, and these were introduced into the trajectory computations. The coefficients are $K_t = .022$ miles^{-1} and $K_n = .020$ miles^{-1}.

The mechanics of the step-wise trajectory technique are outlined in the appendix. The technique pre-supposes that the pressure field is known, or that an average pressure profile representative of the pressure field is available. The pressure field observed in the 1949 Lake Okeechobee hurricane was adopted for the model. In the basic field, the pressure was assumed to be symmetrical with respect to the geometric center, the pressure gradient being given by the relation (Schloemer, /18/):

$$\frac{dp}{dr} = (p_n - p_o)\frac{R}{r^2}e^{-R/r} \qquad (1)$$

The values of p_n, p_o, and R used were 1014 mb., 955 mb., and 22 statute miles respectively, these being averages observed in the Lake Okeechobee hurricane (Myers /14/). A more detailed enumeration of the pressures and pressure gradients in this model pressure field appears in table 1. Air density in the trajectory computations was assumed to be constant at 1.15×10^{-3} gm per cubic centimeter, while a value of .238 hr.$^{-1}$ for Coriolis parameter, corresponding to latitude 27°, was used.

The trajectory technique was tested by constructing trajectories beginning with boundary values at 120 miles radius, with the model pressure field held stationary. It was found that the computed radial profiles of wind speed and deflection angle did simulate the average profiles observed in the storm. This was a test of the trajectory technique only and not of the friction coefficients, as the latter were derived from this same storm.

The manual technique for preparing the trajectories, even with the help of the nomograms described in the appendix, is tedious and time-consuming, requiring painstaking efforts to avoid any error that would preclude checking by construction of a reproducible trajectory. The available manpower and time restricted the construction of trajectories to a relative few. Plans

Table 1. - Parameters for model hurricane

r Radial Distance From Hurricane Center (Statute miles)	p Pressure (inches)	p Pressure (mb.)	$\frac{1}{\rho}\frac{\partial p}{\partial r}$ Pressure Force Per Unit Mass (mi./hr.^{2})	Stationary Storm Equilibrium Wind* Speed (m.p.h.)	Stationary Storm Equilibrium Wind* Deflection Angle (degrees)	Stationary Storm Adjusted Equilibrium Wind Speed (m.p.h.)	Stationary Storm Adjusted Equilibrium Wind Deflection Angle (degrees)
0	28.20	955.0					
10	28.40	961.7	636	71.7	10.0	71.8	8.4
20	28.53	966.1	468	80.2	18.0	79.6	16.9
22	28.85	977.0	429	77.3	20.1	77.5	20.1
25	28.93	979.7	378	76.2	20.8	--	--
30	29.05	983.8	304	71.9	23.1	71.2	30.0
35	29.15	987.1	248	67.4	25.0	--	--
40	29.22	989.5	206	63.1	26.4	61.7	35.3
50	29.34	993.6	147	55.5	28.8	53.8	37.9
60	29.44	997.0	110	49.4	30.4	47.4	39.4
70	29.50	999.0	84	43.7	31.5	41.8	40.0
80	29.55	1000.7	68	39.5	32.2	37.9	40.1
90	29.59	1002.0	56	36.1	32.8	34.8	39.6
100	29.62	1003.0	46	32.7	33.0	31.7	39.0
110	29.65	1004.1	40	30.5	33.2	29.8	38.3
120	29.68	1005.1	34	28.4	33.3	27.6	37.3

*From nomogram, figure 3

are being implemented for programming the numerical computation of the trajectories using one of the smaller electronic digital computers now available.

3. EQUATIONS OF HORIZONTAL MOTION FOR HURRICANE SURFACE LAYER

VECTOR EQUATION. Some of the characteristics of surface winds and wind fields in hurricanes may be surmised from the equations of horizontal motion.

The wind flow near the sea surface in the region of a hurricane outside the wall of the eye is essentially horizontal. The vector equation of horizontal motion which governs this flow is (Haltiner and Martin [4] see especially p. 173):

$$\frac{d\vec{V}}{dt} = -\frac{1}{\rho}\vec{\nabla}_2 p + f\vec{V}\times\vec{k} + \vec{F}. \tag{2}$$

Integrating over a time interval from t_1 to t_2:

$$\vec{V}_2 - \vec{V}_1 = \left[-\overline{\frac{1}{\rho}\vec{\nabla}_2 p} + \overline{f\vec{V}\times\vec{k}} + \vec{F}\right](t_2 - t_1). \tag{3}$$

The bars in equation 3 represent averages over the time interval $t_2 - t_1$.

For convenience we introduce into (3) the vector definition of the geostrophic wind:

$$f\,\vec{V}_g\times\vec{k} = \frac{1}{\rho}\vec{\nabla}_2 p, \tag{4}$$

which yields

$$\vec{V}_2 - \vec{V}_1 = \left(\overline{-f\vec{V}_g\times\vec{k}} + \overline{f\vec{V}\times\vec{k}} + \vec{F}\right)(t_2 - t_1) = f\left[\overline{(\vec{V} - \vec{V}_g)\times\vec{k}}\right](t_2 - t_1) + \vec{F}(t_2 - t_1). \tag{5}$$

These vectors are shown schematically in figure 1. The trajectory technique adapted from Goodyear [3] and described in the appendix is a graphical stepwise solution of equation (5).

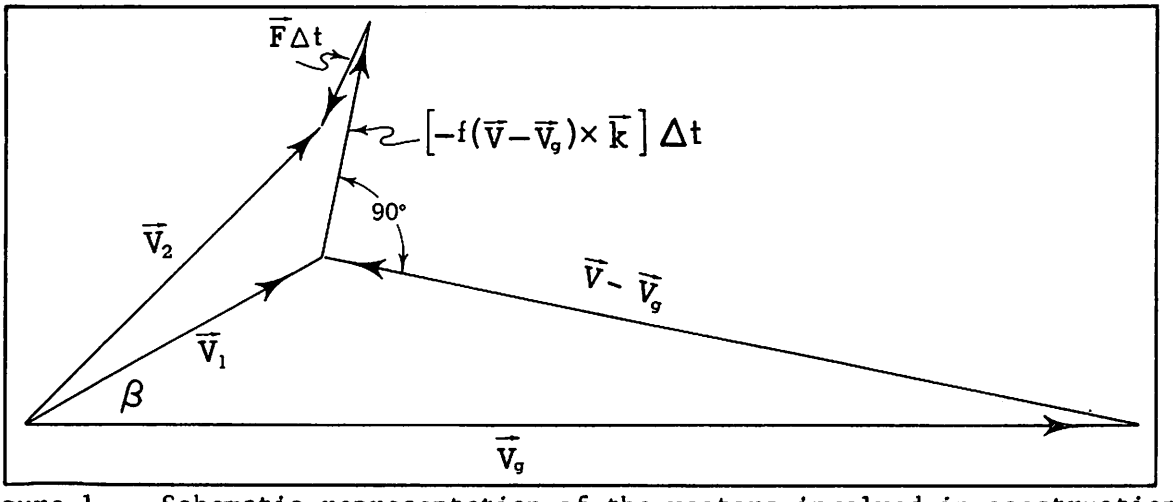

Figure 1. - Schematic representation of the vectors involved in construction of the trajectories (see equation (5)).

SCALAR EQUATIONS. Insight into the factors controlling the average horizontal motions in the hurricane surface wind field is obtained by use of the scalar components of (2). These components, tangential and normal to the trajectory of the air, respectively are

$$\frac{dV}{dt} = -\frac{1}{\rho}\frac{\partial p}{\partial s} - F_t \tag{6}$$

$$V\frac{d\alpha}{dt} = -\frac{1}{\rho}\frac{\partial p}{\partial n} + fV + F_n. \tag{7}$$

Several substitutions and transformations in (6) and (7) prove to be useful. The frictional accelerations are related to the speed, according to studies by Myers [15]. It was empirically determined in the August 26, 1949 hurricane over the waters of Lake Okeechobee, Fla., that

$$F_t = K_t V^2;\ F_n = K_n V^2 \tag{8}$$

where K_t and K_n are empirical constants with dimensions of length^{-1}.

A transformation is now made to a polar coordinate system centered at and moving with the center of the model hurricane. In this system (see fig. 2) the position variables are the radius vector, r, and the azimuth, θ, positive clockwise from the direction of motion of the storm (conforming to meteorological instead of mathematical convention with respect to sign). Gradients in the s, n, r, and θ directions of any variable, X, are related by the standard forms

$$\frac{\partial X}{\partial s} = -\frac{\partial X}{\partial r}\sin\beta - \frac{1}{r}\frac{\partial X}{\partial \theta}\cos\beta$$

$$\frac{\partial X}{\partial n} = \frac{\partial X}{\partial r}\cos\beta - \frac{1}{r}\frac{\partial X}{\partial \theta}\sin\beta \tag{9}$$

Thus,

$$\frac{\partial p}{\partial s} = -\frac{\partial p}{\partial r}\sin\beta - \frac{1}{r}\frac{\partial p}{\partial \theta}\cos\beta;\ \frac{\partial p}{\partial n} = \frac{\partial p}{\partial r}\cos\beta - \frac{1}{r}\frac{\partial p}{\partial \theta}\sin\beta \tag{10}$$

The next substitution is to replace the absolute value of the wind direction, α, in equation (7) by variables more suited to a quasi-symmetrical system. From figure 2,

$$\alpha = \theta - \beta + 90°. \tag{11}$$

Differentiating,

$$\frac{d\alpha}{dt} = -\frac{d\beta}{dt} + \frac{d\theta}{dt}. \tag{12}$$

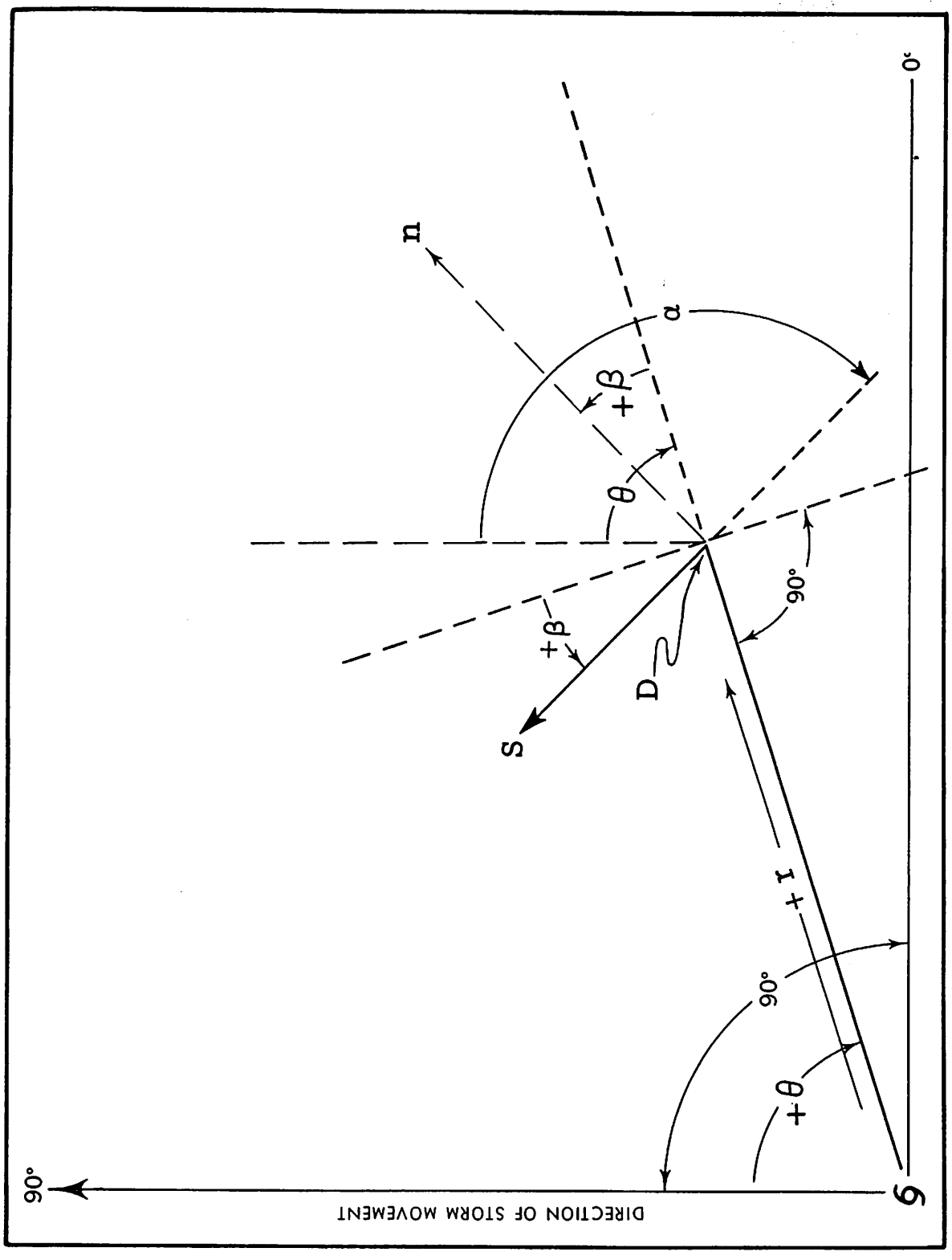

Figure 2. - Angles and vector displacements used to describe the wind at a point D, in a hurricane field (see list of symbols for further details).

Finally, relations of acceleration to velocity and gradient of velocity (equations (17) and (19) below) are obtained from the expressions for the total derivatives. Since V and β are functions of r, θ, and t only, we can write:

$$\frac{dV}{dt} = \frac{\partial V}{\partial r}\frac{dr}{dt} + \frac{\partial V}{\partial \theta}\frac{d\theta}{dt} + \frac{\partial V}{\partial t}$$
$$\frac{d\beta}{dt} = \frac{\partial \beta}{\partial r}\frac{dr}{dt} + \frac{\partial \beta}{\partial \theta}\frac{d\theta}{dt} + \frac{\partial \beta}{\partial t} \tag{13}$$

Here dr/dt is the total time rate of change of the distance from the storm center to an air parcel. But

$$\frac{dr}{dt} = \left(\frac{dr}{dt}\right)_1 + \left(\frac{dr}{dt}\right)_2 \tag{14}$$

where $(dr/dt)_1$ is the rate of change of length r due to motion of the air parcel and $(dr/dt)_2$ is the change in r due to motion of the storm center. From geometrical considerations:

$$\left(\frac{dr}{dt}\right)_1 = -V \sin\beta; \quad \left(\frac{dr}{dt}\right)_2 = -V_H \cos\theta. \tag{15}$$

By similar reasoning,

$$\frac{d\theta}{dt} = \left(\frac{d\theta}{dt}\right)_1 + \left(\frac{d\theta}{dt}\right)_2 = -\frac{V}{r}\cos\beta + \frac{V_H}{r}\sin\theta. \tag{16}$$

Now substituting (8) and (10) into the right-hand side of equation (6), and (13) thru (16) for the left-hand side, yields the expanded tangential equation,

$$\frac{dV}{dt} = -\frac{\partial V}{\partial r}(V\sin\beta + V_H\cos\theta) + \frac{1}{r}\frac{\partial V}{\partial \theta}(V_H\sin\theta - V\cos\beta) + \frac{\partial V}{\partial t}$$
$$= \frac{1}{\rho}\frac{\partial p}{\partial r}\sin\beta + \frac{1}{\rho r}\frac{\partial p}{\partial \theta}\cos\beta - K_t V^2 \tag{17}$$

The same substitutions in equation (7) together with the following combination of (12) and (16)

$$\frac{d\alpha}{dt} = -\frac{d\beta}{dt} - \frac{V}{r}\cos\beta + \frac{V_H}{r}\sin\theta, \tag{18}$$

yield the expanded normal equation

$$V\frac{d\beta}{dt} = -V\frac{\partial \beta}{\partial r}(V\sin\beta + V_H\cos\theta) + \frac{V}{r}\frac{\partial \beta}{\partial \theta}(V_H\sin\theta - V\cos\beta) + V\frac{\partial \beta}{\partial t}$$
$$= \frac{1}{\rho}\frac{\partial p}{\partial r}\cos\beta - \frac{1}{\rho r}\frac{\partial p}{\partial \theta}\sin\beta - fV - \frac{V^2}{r}\cos\beta + \left(\frac{V}{r}\right)V_H\sin\theta - K_n V^2. \tag{19}$$

It is worthy of note that V^2/r_T, the total centrifugal force, is divided into three parts in equation (19). $(V^2/r)\cos\beta$ is that part of V^2/r_T that must be overcome to maintain a constant deflection angle in a stationary storm, while $-(V/r)V_H\sin\theta$ is the additional centrifugal force that must be overcome to maintain a constant deflection angle in the moving storm. The remaining portion of V^2/r_T is available to modify the deflection angle and is symbolized by $V(d\beta/dt)$.

The only restriction on the generality of equations (17) and (19) for expressions governing the horizontal components of motion is that the relation of the frictional stress to speed be as stated in equation (8). The θ-gradients of pressure are generally of a lower order of magnitude than the r-gradients, the frictional accelerations, or the centrifugal acceleration, even in hurricanes with appreciable asymmetry of the pressure field, and may be neglected in most applications of the above equations.

For a permanent-state hurricane in which the isotach and isogon fields move forward without change at the velocity, V_H, of the pressure field, and with the coordinate system also moving with the storm, the terms $\partial V/\partial t$ and $V(\partial\beta/\partial t)=0$. For a stationary steady-state symmetrical storm (17) and (19) reduce to:

$$\frac{dV}{dt} = -V\frac{\partial V}{\partial r}\sin\beta = \frac{1}{\rho}\frac{\partial p}{\partial r}\sin\beta - K_t V^2 \tag{20}$$

$$V\frac{d\beta}{dt} = -V^2\frac{\partial\beta}{\partial r}\sin\beta = \frac{1}{\rho}\frac{\partial p}{\partial r}\cos\beta - fV - \frac{V^2}{r}\cos\beta - K_n V^2. \tag{21}$$

4. EQUILIBRIUM WIND

The extensive utility of the geostrophic wind in approximating frictionless flow of little curvature prompted the idea of defining a counterpart wind vector representing a balance of forces in the hurricane surface wind field. This concept was indeed found useful and the vector was named the equilibrium wind. It is defined as that value of the wind speed and direction at a particular point in a hurricane pressure field such that $dV/dt=0$ and $d\beta/dt=0$ in equations (17) and (19). Momentarily there would be no change in speed or in deflection angle if the wind vector were equal to the equilibrium value. The gradient wind, as defined by the conventional gradient wind equation, is a particular case of the equilibrium wind in which K_t, K_n, and β are zero; r is so chosen that $\partial p/\partial\theta=0$; and V_H is neglected. Another particular case is for uniform unaccelerated flow over the sea at an angle to straight isobars, a condition closely approximated in much wind flow over the ocean. In this latter example r equals infinity and $V_H = 0$.

The EQUILIBRIUM WIND EQUATIONS, from (17) and (19) are

$$\frac{1}{\rho}\frac{\partial p}{\partial r}\sin\beta_b + \frac{1}{\rho r}\frac{\partial p}{\partial \theta}\cos\beta_b - K_t V_b^2 = 0 \tag{22}$$

$$\frac{1}{\rho}\frac{\partial p}{\partial r}\cos\beta_b - \frac{1}{\rho r}\frac{\partial p}{\partial \theta}\sin\beta_b - fV_b - \frac{V_b^2}{r}\cos\beta_b - K_n V_b^2 + \frac{V_b V_H}{r}\sin\theta = 0. \tag{23}$$

Simultaneous solution of (22) and (23) will yield values of V_b and β_b at any point in a model or observed hurricane, for assumed values of K_t and K_n and observed or assumed values of the pressure gradient and V_H.

EQUILIBRIUM WIND FOR MODEL HURRICANE. The most simple application of the equilibrium wind is to estimate the surface wind associated with a symmetrical stationary pressure field by simultaneous solution of

$$\frac{1}{\rho}\frac{\partial p}{\partial r}\sin\beta_b - K_t V_b^2 = 0 \tag{24}$$

$$\frac{1}{\rho}\frac{\partial p}{\partial r}\cos\beta_b - fV_b - \frac{V_b^2}{r}\cos\beta_b - K_n V_b^2 = 0. \tag{25}$$

A nomogram is shown in figure 3 from which one may make this computation for the model hurricane described in section 2. The intersection is found between the arc corresponding to the pressure gradient force and the sloping line corresponding to the radius. Then V_β and β_b are read as indicated in the insert. The resulting equilibrium wind values for the stationary case are shown in table 1.

The effect of storm movement on the equilibrium wind is illustrated (table 2) by repeating the solutions for two values of storm speed, V_H, thus including the last term of equation (23). A direct numerical solution of (22) and (23) was used, the nomogram of figure 3 being valid only for a stationary storm. The equilibrium wind speeds are everywhere higher to the right of the storm than at corresponding points in the left semicircle. However, the differences in speed are small at a radius of 120 miles and get gradually larger as the distance from the center decreases. The differences are magnified somewhat in the faster moving storm. The largest speed differences at corresponding points in the right and left semicircles occurred in the 30 m.p.h. hurricane, near the radius of maximum winds, the speed on the right being approximately 130 percent of the speed to the left. Deflection angles decrease with decreasing distance from the center, the rate of decrease being greatest on the inside of the radius of maximum winds. The 30 m.p.h. hurricane deflection angles are greater than those in the 10 m.p.h. hurricane in the right semicircle, while the reverse holds in the left semicircle.

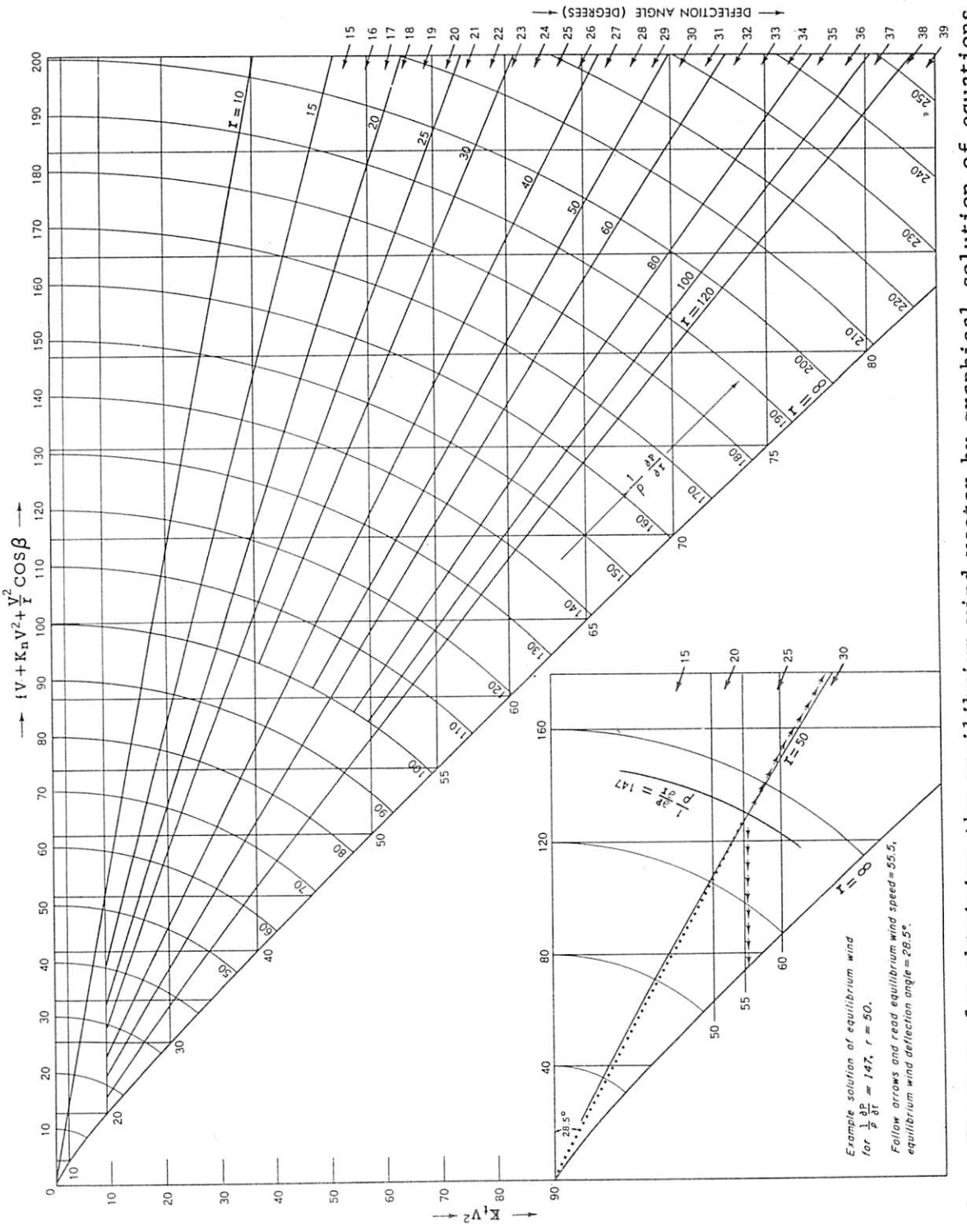

Figure 3. - Nomogram for obtaining the equilibrium wind vector by graphical solution of equations (24) and (25).

Table 2. - Equilibrium wind values in a moving, model hurricane

r	θ	0°, 180°		30°, 150°		60°, 120°		90°		210°, 330°		240°, 300°		270°	
		V_b	β_b	V_b	β_b	V_b	β_b	V_b	β_b	V_b	β_b	V_b	β_b	V_b	β_b
10		71.7	10.2	73.8	10.9	75.4	11.3	76.0	11.5	69.7	9.7	68.2	9.3	67.7	9.1
		71.7	10.2	78.2	12.2	83.4	13.9	85.4	14.6	65.8	8.6	61.8	7.6	60.4	7.3
20		79.5	17.3	81.3	18.1	82.6	18.7	83.1	18.9	77.8	16.5	76.5	16.0	76.1	15.8
		79.5	17.3	84.9	19.8	89.3	22.0	90.9	22.8	74.4	15.1	71.0	13.7	69.8	13.2
22		78.4	18.4	80.1	19.2	81.4	19.9	81.9	20.1	76.8	17.6	75.6	17.0	75.1	16.8
		78.4	18.4	83.7	21.0	87.9	23.3	89.5	24.2	73.6	16.1	70.2	14.6	69.0	14.1
25		76.5	19.9	78.1	20.8	79.4	21.5	79.8	21.8	74.9	19.1	73.8	18.5	73.4	18.3
		76.5	19.9	81.5	22.7	85.5	25.2	87.0	26.1	71.9	17.5	68.7	15.9	67.6	15.4
30		72.1	22.0	73.6	23.0	74.7	23.8	75.1	24.1	70.6	21.2	69.6	20.5	69.2	20.3
		72.1	22.0	76.7	25.2	80.3	27.8	81.7	28.9	67.8	19.4	64.9	17.7	63.9	17.2
35		67.6	23.8	69.0	24.9	70.0	25.7	70.4	26.0	66.2	23.0	65.3	22.2	64.9	22.0
		67.6	23.8	71.8	27.2	75.1	30.0	76.4	31.2	63.6	21.0	60.9	19.2	60.0	18.6
40		63.4	25.4	64.6	26.5	65.6	27.3	65.9	27.6	62.1	24.4	61.2	23.7	60.9	23.4
		63.4	25.4	67.3	28.9	70.3	31.8	71.5	33.1	59.7	22.4	57.2	20.4	56.3	19.8
50		55.7	27.6	56.8	28.8	57.6	29.7	57.9	30.0	54.6	26.6	53.9	25.8	53.6	25.5
		55.7	27.6	59.0	31.4	61.6	34.6	62.6	35.9	52.6	24.5	50.4	22.3	49.6	21.6
60		49.4	29.2	50.3	30.4	51.0	31.4	51.3	31.6	48.5	28.0	47.8	27.3	47.6	26.9
		49.4	29.2	52.3	33.2	54.5	36.4	55.3	37.7	46.7	25.9	44.8	23.7	44.1	22.9
80		39.9	30.9	40.6	32.3	41.1	33.2	41.3	33.5	39.1	29.7	38.6	28.9	38.4	28.6
		39.9	30.9	42.1	35.0	43.8	38.4	44.4	39.6	37.7	27.4	36.3	25.2	35.7	24.4
100		33.1	31.6	33.7	33.0	34.2	34.0	34.3	34.2	32.5	30.5	32.1	29.6	32.0	29.3
		33.1	31.6	34.9	35.6	36.3	39.1	36.8	40.4	31.4	28.1	30.2	25.9	29.7	25.0
120		28.6	31.9	29.1	33.1	29.4	34.1	29.6	34.3	28.1	30.6	27.7	29.9	27.6	29.5
		28.6	31.9	30.1	35.9	31.2	39.0	31.6	40.2	27.1	28.4	26.1	26.2	25.7	25.3

r = radial distance from hurricane center (statute miles);
θ = azimuth angle (degrees);
V_b = equilibrium wind speed (m.p.h.);
β = equilibrium deflection angle (degrees)

Upper figures for hurricane moving 10 m.p.h., lower figures for hurricane moving 30 m.p.h. Values determined by numerical solution of equations (22) and (23).

The $\partial p/\partial\theta$ terms of (22) and (23) were equal to zero in the above computations because of the symmetrical nature of the model pressure field. However, as indicated previously, for hurricane pressure fields with the usual degree of asymmetry these terms would still be small in comparison to the other terms and for most purposes could reasonably be neglected in equilibrium wind evaluations.

ADJUSTED EQUILIBRIUM WIND. For a stationary hurricane, a further step may be taken in developing a dynamic description of the wind field by taking into account the acceleration of the air inward along r. A field of equilibrium wind vectors reveals a variation of V along a trajectory, yet is derived from the assumption that $dV/dt = 0$. One means of obtaining a wind field that is dynamically consistent with a given pressure field is to adjust the equilibrium wind the minimum amount required to yield compatible values of dV/dt and $V(d\beta/dt)$ in the equations of horizontal motion. This adjusted equilibrium wind is readily obtained to a close degree of approximation for a stationary symmetrical storm.

While the adjusted equilibrium wind will differ somewhat from the equilibrium wind, the radial gradients of the two can differ very little. (For an example of a comparison, see fig. 6). We therefore assume

$$\frac{\partial V'}{\partial r} = \frac{\partial V_b}{\partial r} \quad , \quad \frac{\partial \beta'}{\partial r} \frac{\partial \beta_b}{\partial r} \tag{26}$$

where the primes refer to the adjusted equilibrium wind. Substitution in (20) and (21) yields the adjusted equilibrium wind equations,

$$-V' \frac{\partial V_b}{\partial r} \sin \beta' = \frac{1}{\rho} \frac{\partial p}{\partial r} \sin \beta' - K_t V'^2 \tag{27}$$

$$-V'^2 \frac{\partial \beta_b}{\partial r} \sin \beta' = \frac{1}{\rho} \frac{\partial p}{\partial r} \cos \beta' - fV' - \frac{V'^2}{r} \cos \beta' - K_n V'^2 \tag{28}$$

The adjusted equilibrium wind is obtained by first solving for the equilibrium wind at various radii, obtaining the radial gradients, $\partial V_b/\partial r$ and $\partial \beta_b/\partial r$, and substituting these into (27) and (28). Equations (27) and (28) are then solved simultaneously for V' and β'.

The adjusted equilibrium wind values for the model hurricane may be compared with the equilibrium wind in table 1 and figure 6.

5. FRICTIONAL DAMPING

In both nature and machines a common behavior of friction is to damp motions toward some particular velocity. This occurs where there is an interrelation between the frictional acceleration and the speed and where at least one of the applied forces is not small in comparison with the other applied forces and is independent of the speed. The strong frictional accelerations on hurricane winds at the sea surface play this role and everywhere

tend to damp the wind toward an equilibrium value. That the winds are indeed so damped will be illustrated by examples from trajectories in the model hurricane.

Trajectories were computed through the model pressure field from differing initial velocities at a radius of 120 miles by the graphical techniques based on equation (5). The equilibrium wind at this radius has a speed of 28.4 m.p.h. and a deflection angle of 33.3°. Different speeds were introduced at this radius, at the equilibrium deflection angle. The respective speeds from the trajectories are graphed in figure 4.

Note how the profiles having initial wind speeds that are too high for equilibrium overshoot toward lower values. In analogous fashion, the profile of the trajectory with too low an initial speed overshoots toward high values. Rapid damping of the oscillations brings the profiles into approximate coincidence with each other long before they reach the radius of maximum winds.

The corresponding deflection angle profiles for the same trajectories are portrayed in figure 5. The amplitude of the oscillations is large, but again damping is effective in bringing the profiles together. The oscillations are grouped around the profile based on the trajectory having for its initial velocity the value of the equilibrium wind at the respective radius.

The significance of the computed equilibrium wind, and especially the adjusted equilibrium wind, as values toward which the wind in the friction layer is damped, is pictured in figure 6. In this figure are shown coincident plots of (a) the trajectory-derived wind profile from figure 4 which experienced the fewest oscillations, (b) the equilibrium wind, (c) the adjusted equilibrium wind, and (d) the smoothed over-water observed wind profile in the hurricane from which the friction coefficients and pressure field parameters were derived (1949, Lake Okeechobee, Fla.) The deviation of the trajectory-based wind profile from the adjusted equilibrium wind, due to the effect of approximations in the graphical trajectory technique, has not been determined.

Further understanding of the manner in which frictional damping takes place is gained by comparing the forces that change the wind speed. Equation (6) is a convenient expression of these forces. Each of the three terms of equation (6) has been plotted independently against lapsed time in figure 7 for the case of initial speed of 34 m.p.h. in figure 4. Note that the pressure gradient force along the trajectory decreases slightly during the first hour, because an initial wind somewhat stronger than the equilibrium speed was introduced at the periphery. The wind immediately turns to a smaller deflection angle (fig. 5). Sine β of equation (10) decreases more rapidly than $\partial p/\partial r$ increases, for a short time, giving a net decrease in $\partial p/\partial s$.

Subsequently, the increase in the pressure gradient force is nearly matched by the increase in the frictional retardation. Consequently,

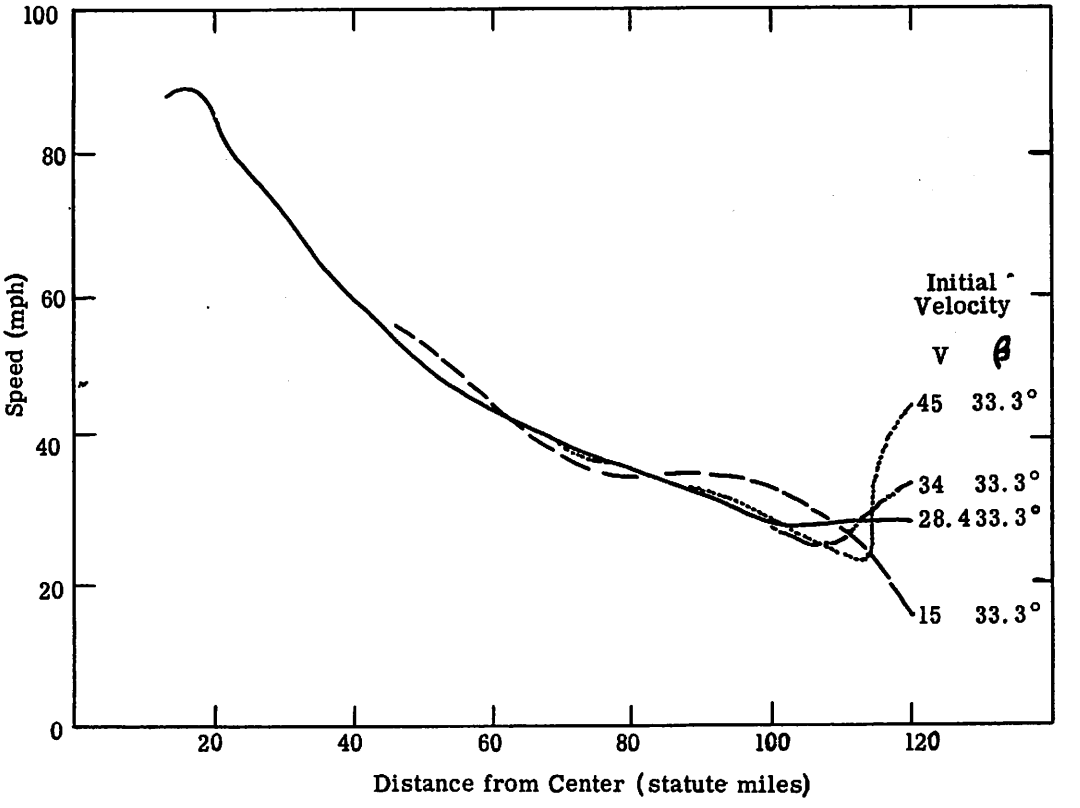

Figure 4. - Surface wind speeds in stationary hurricane with differing initial velocities.

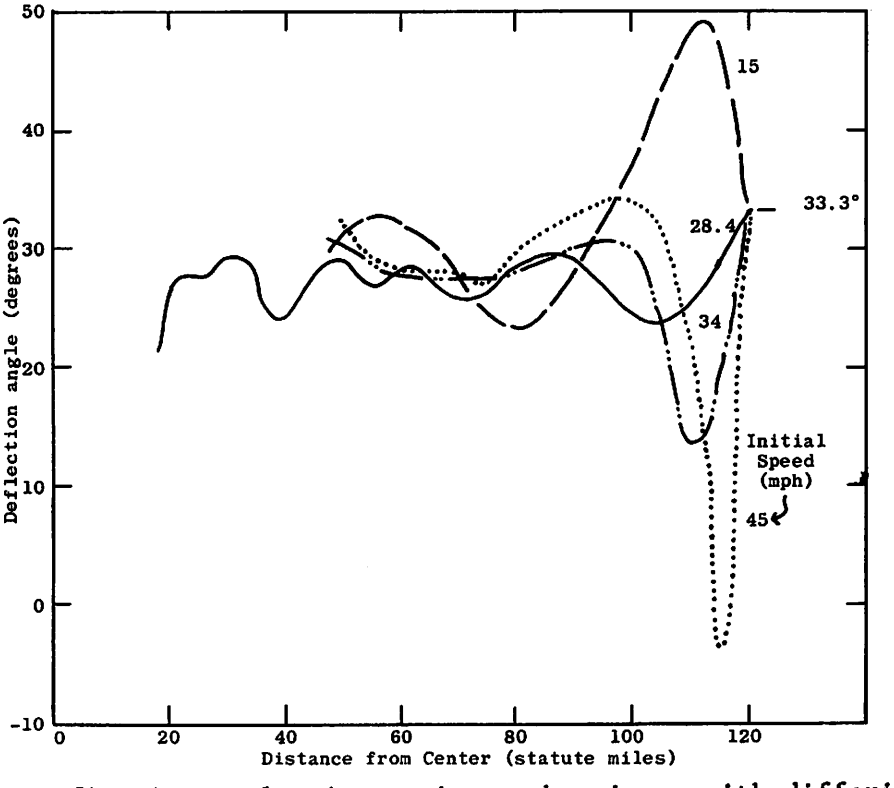

Figure 5. - Deflection angles in stationary hurricane with differing initial velocities.

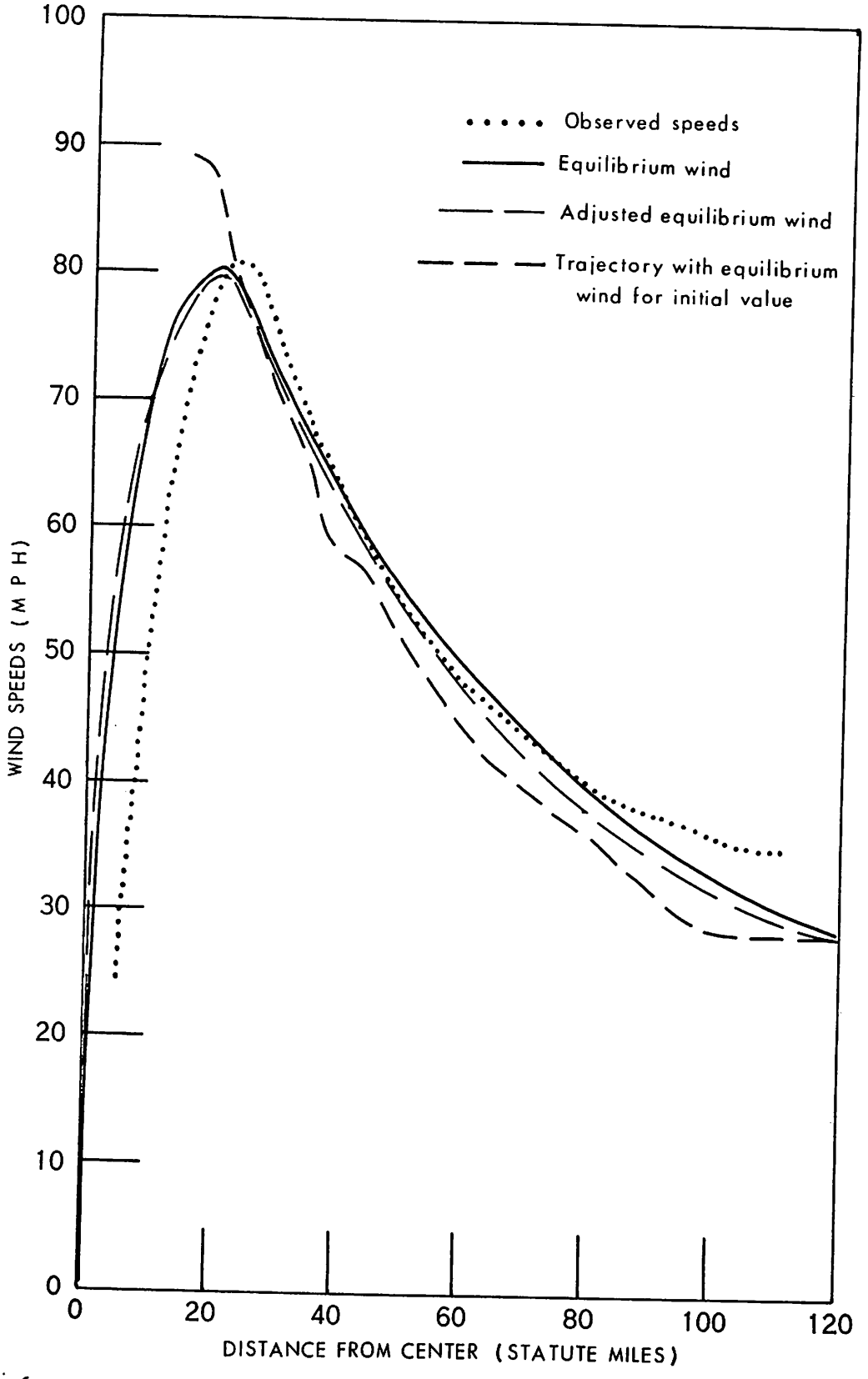

Figure 6. - Average observed speed profile in hurricane of August 26, 1949 and some computed profiles.

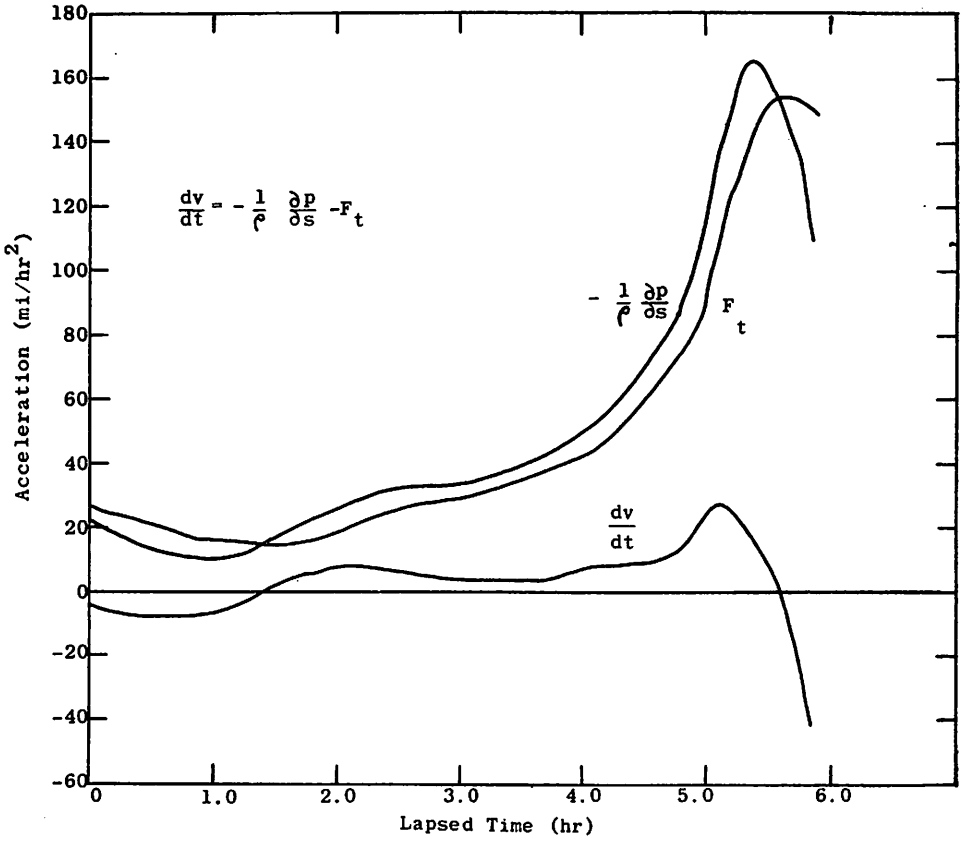

Figure 7. - Accelerations along trajectory in stationary hurricane.

the values of net acceleration remain fairly constant and rather low. The frictional force, being directly proportional to the square of the speed, and acting opposite to the component of the pressure gradient along the trajectory, keeps the resultant acceleration within moderate bounds.

The final conclusion of this section is that peripheral velocity asymmetries of the hurricane surface wind are quickly damped out and have little effect on the major part of the surface wind field.

6. EFFECTS OF A MOVING PRESSURE FIELD

A question of great interest is the effect of motion of a hurricane on the surface wind field. The winds are usually observed to be stronger in some parts of the right half of a moving hurricane than at corresponding locations in the left half. The dynamic effect of motion per se on the surface winds derives from the motion of the pressure field. Air in the front of a moving hurricane encounters a stronger pressure gradient more quickly and air in the rear less quickly than in a stationary storm for the same air velocity.

The equilibrium wind (table 2) portrays the above-described asymmetry. However, as previously pointed out, a field of the equilibrium wind is

dynamically inconsistent. The device of the adjusted equilibrium wind, by which a solution for the equations of horizontal motion was obtained for a stationary storm, was not extended to the moving storm. In that technique, radial gradients of the equilibrium wind were substituted for radial gradients of the adjusted equilibrium wind. There is less basis for equating the θ-gradients of equilibrium and adjusted equilibrium winds; such a step it was feared might impose a solution of the equations in which the asymmetry of the wind was artifically restricted.

Conclusions on the effect of storm motion were therefore based on sample cases from computed trajectories. The asymmetry and other effects described in this section are attributed solely to the influence of storm motion.

Wind fields were obtained by analysis of point values of speed and deflection angles obtained by manual construction of three sets of trajectories through the model pressure field moving at 10, 20 and 30 m.p.h. In each instance, 12 trajectories were constructed to provide the data for each respective wind field. The individual trajectories of each set originated 120 miles from the center. Other initial conditions were speed 34 m.p.h. and deflection angle 33°. The pressure field was held constant and also symmetrical with respect to the center, the prevailing pressure gradient being given by equation (1). For the case of a stationary storm, one trajectory sufficed to define the wind field.

The traces of the trajectories for the 10 m.p.h. storm with respect to the surface, superimposed on one another, are shown in figure 8. The trajectories when plotted with respect to the moving center, for all the storms, are shown in figure 9. The trajectory field for the stationary storm of figure 9 is similar to the average trajectories shown by Hughes(8 see especially p. 425).

A comparison between the speed of the storm and the number of trajectories that spiral in toward the center is shown in table 3.

Table 3. - Comparison between speed of storm and number of trajectories spiralling in toward center

Total Number of Trajectories in Set	Number of Trajectories That do not Spiral in Toward Center	Speed of Storm (m.p.h.)
12	0	Stationary
12	2	10
12	6	20
12	8	30

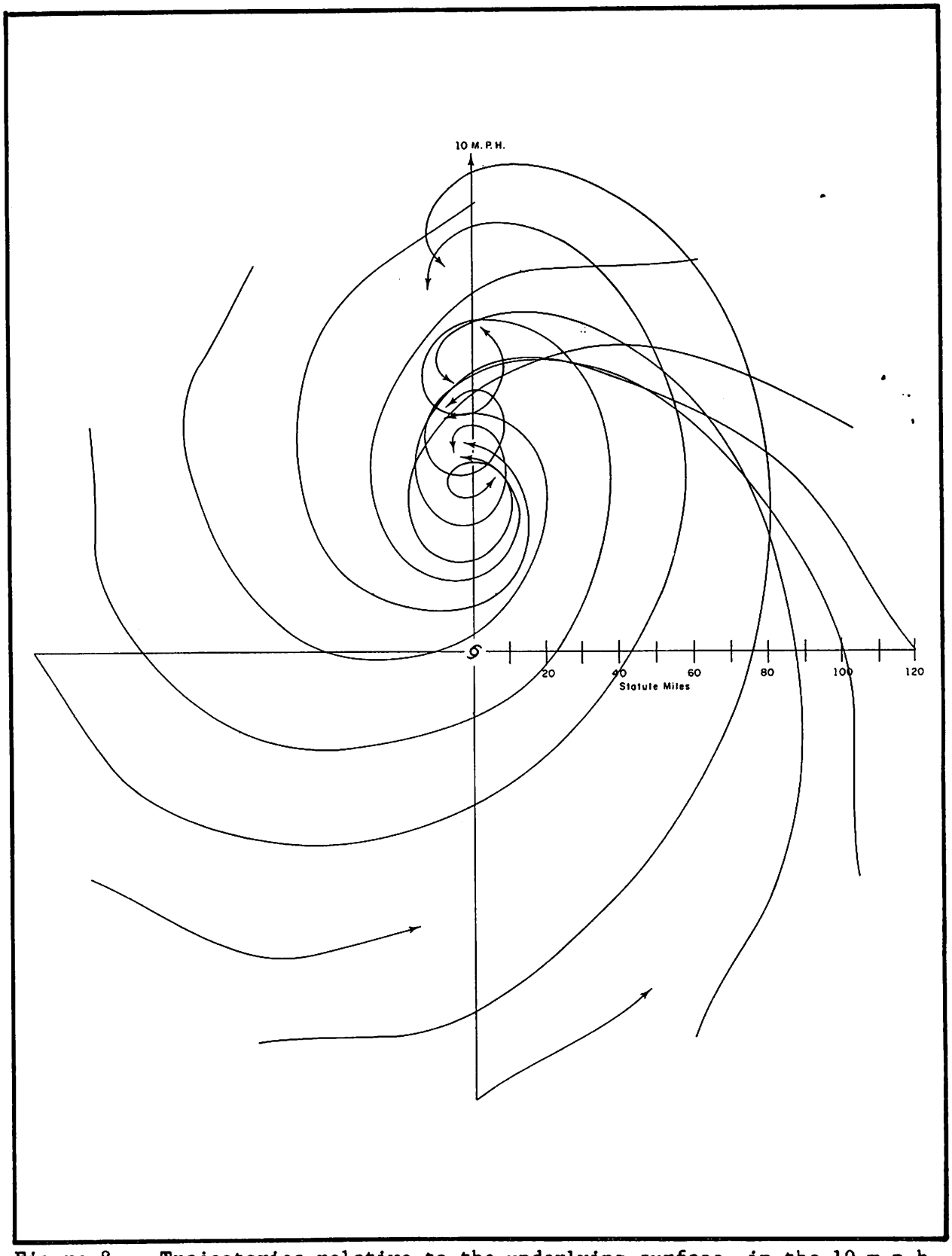

Figure 8. - Trajectories relative to the underlying surface, in the 10 m.p.h. hurricane.

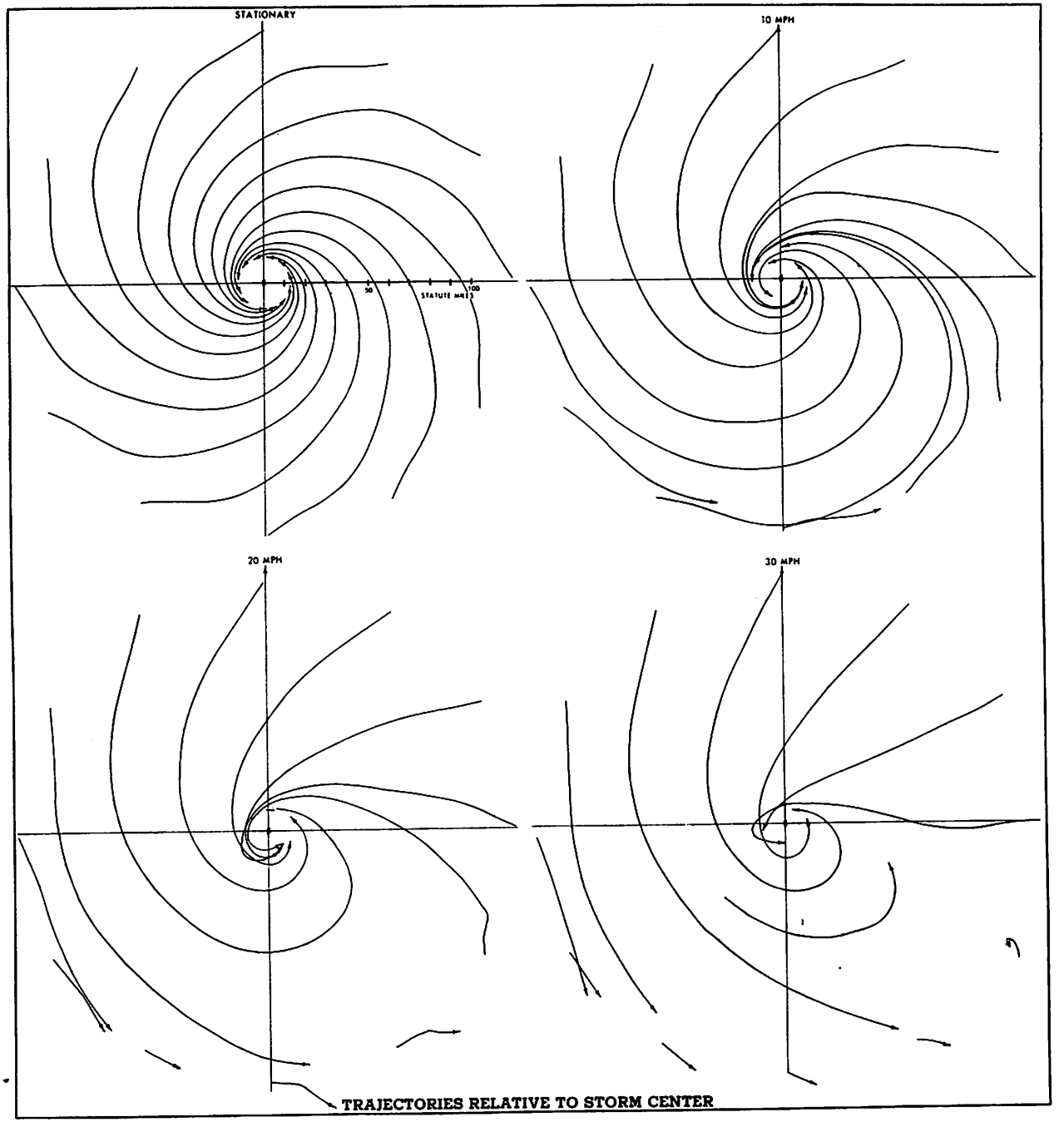

Figure 9. - Trajectories relative to the storm center in model hurricane moving at different speeds.

We may conclude from table 3, or by inspection of the trajectory fields (fig. 9), that as the speed of the storm increases, the area over which the paths of air parcels fail to spiral inward also increases. As a corollary, we may infer that the greater the speed of the storm the greater the exchange of air per unit time between the storm and its environment. We would then expect that modifications such as filling, in a storm that remains tropical in structure, would proceed at a higher rate as the speed of translation increased, other factors being neglected. This hypothesis was born out in a study of filling (Malkin [12]), wherein Hazel of October 1954 was the exceptional storm out of a total of 13 storms studied, moving at a phenomenal rate and simultaneously filling at a rate that appeared unrealistic when compared to the other 12 storms.

Further examination of the trajectory fields (fig. 9) discloses that the trajectories that approached the zone of maximum winds along the shortest paths originated to the right of the storm center. This observation is consistent with Hughes' findings [8] that air parcels from the right front quadrant require the least time to approach the center, and leads to the speculation that, considering the outer portions of the storm, the air to the right is most closely associated with the modifications occurring near the radius of maximum winds and the center.

The trajectory for the stationary storm had a radius of maximum winds of 22 statute miles. This was the average value obtained from the Lake Okeechobee data. The radius varied in the moving storms from:

(a) 13 to 20 miles in the 10 m.p.h. hurricane
(b) 11 to 18 miles in the 20 m.p.h. hurricane
(c) 8 to 20 miles in the 30 m.p.h. hurricane

In each of the moving storms, the radius of maximum winds varied throughout a range equal to roughly half of the value of the average radius of maximum winds. Any hypothesis concerning the variation of the radius of maximum winds with storm movement would consequently be premature at this stage.

An intriguing item concerns the conditions or factors that distinguish between a trajectory that moves in toward the center and one that does not. The radial component of the acceleration of a parcel at a given point in the wind field may be determined using an expression derived from equations (14) and (15):

$$\frac{dr}{dt} = -V \sin \beta - V_H \cos \theta \qquad (29)$$

The field of dr/dt in mi./hr. for the 30 m.p.h. hurricane, is shown in figure 10. The area with negative values (toward the center) has a maximum near the radius of maximum winds in the right front quadrant. Positive values of dr/dt (where air parcels have a component of velocity away from the center,

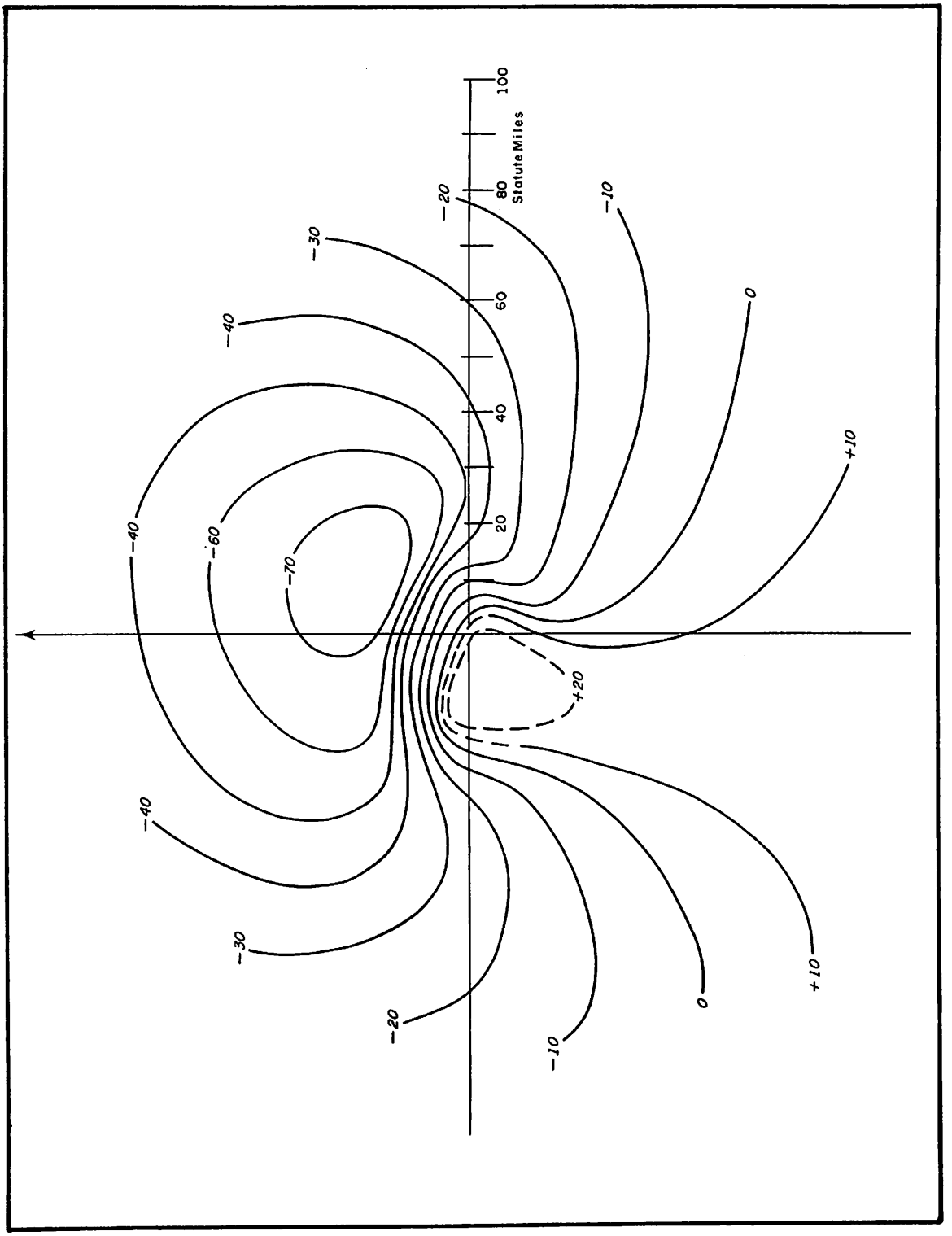

Figure 10. - Field of dr/dt (m.p.h.) for the 30 m.p.h. hurricane.

i.e., are being left behind) are of distinctly lower magnitude than the negative rates observed in the right front quadrant. The positive values are confined to a smaller areal extent in the rear of the storm.

The isotach fields corresponding to uniform motion of the model pressure field are shown in figure 11. An examination of these fields indicates several features of interest:

1. In the moving storms, the highest speeds occur in the right forward quadrant.
2. The higher speeds are found in the faster moving storms.
3. The wind speeds at points directly to the right of the center are only slightly higher than speeds at corresponding distances to the left of the center, the differences being generally very much less than twice the speed of the storm. The actual differences in wind speed, for any point in the field, between the moving and stationary storm, have been depicted in figure 12.

Some averaged fields of radial, tangential, and total wind speeds in tropical storms were computed by Hughes [8], and it is of interest to find that the significant features are reasonably consistent with the isotach fields of figure 11. In making the comparison, it is important to note that the scale in degrees of latitude, as used by Hughes, cannot be expected to show as much detail as the scale in our figures, which is in statute miles, and the wind fields cover an area somewhat less than 2° of latitude from the center.

The deflection angle fields corresponding to the previous isotach and trajectory fields are shown in figure 13. Several features appear to be characteristic and worthy of mention:

1. The largest positive deflection angles are found in the right-front quadrant.
2. Negative (outflow) values of the deflection angle were found in the semicircle to the left of the track and within the radius of maximum winds.
3. The field of deflection angles shows considerable asymmetry in any one storm.
4. The range of deflection angle values computed was greater, the higher the speed of the storm or, looking at this in another way, extreme values of both outflow and inflow were more prevalent, the faster the speed of the storm.

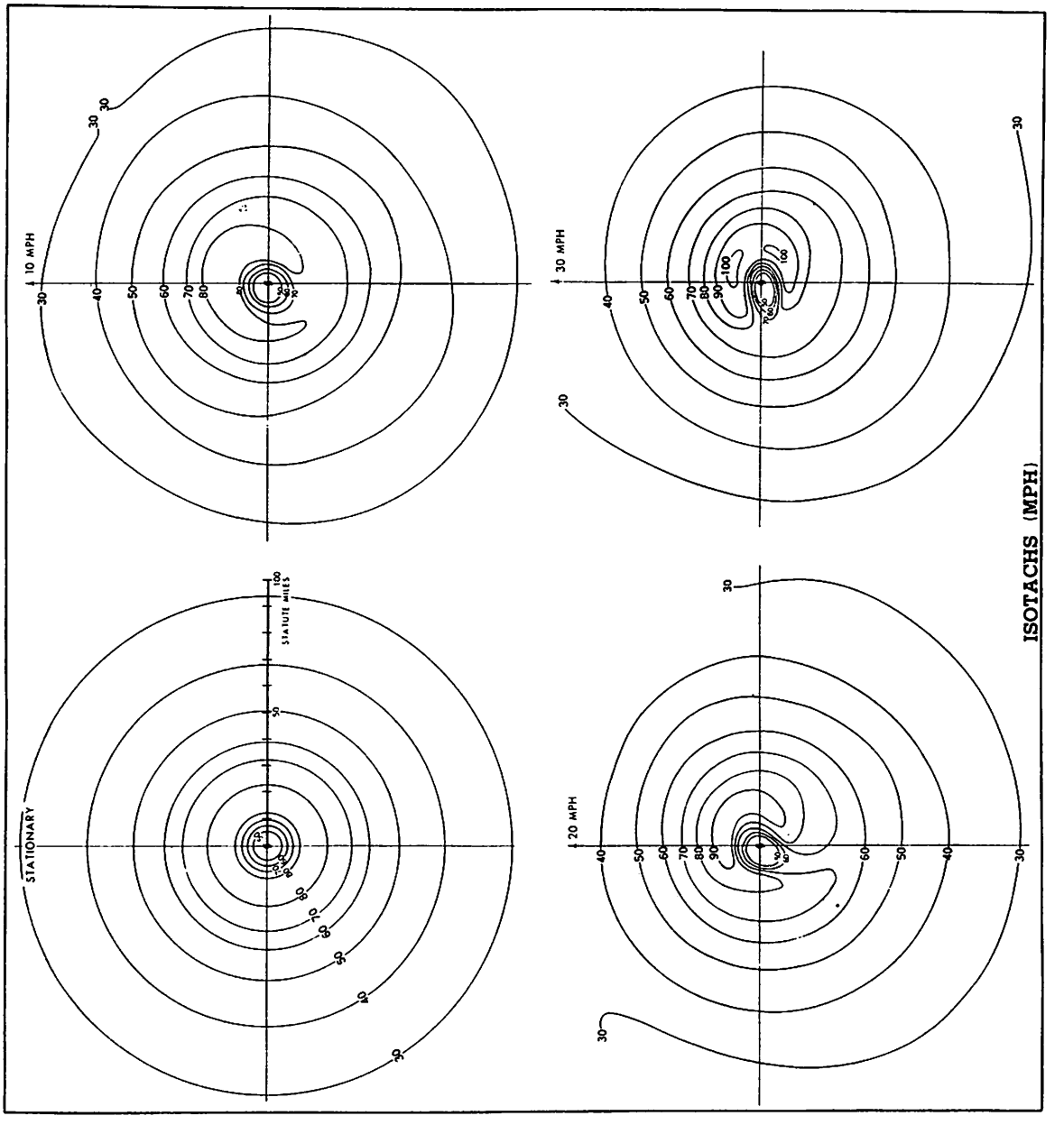

Figure 11. - Isotachs (m.p.h.). Same hurricanes as figure 9.

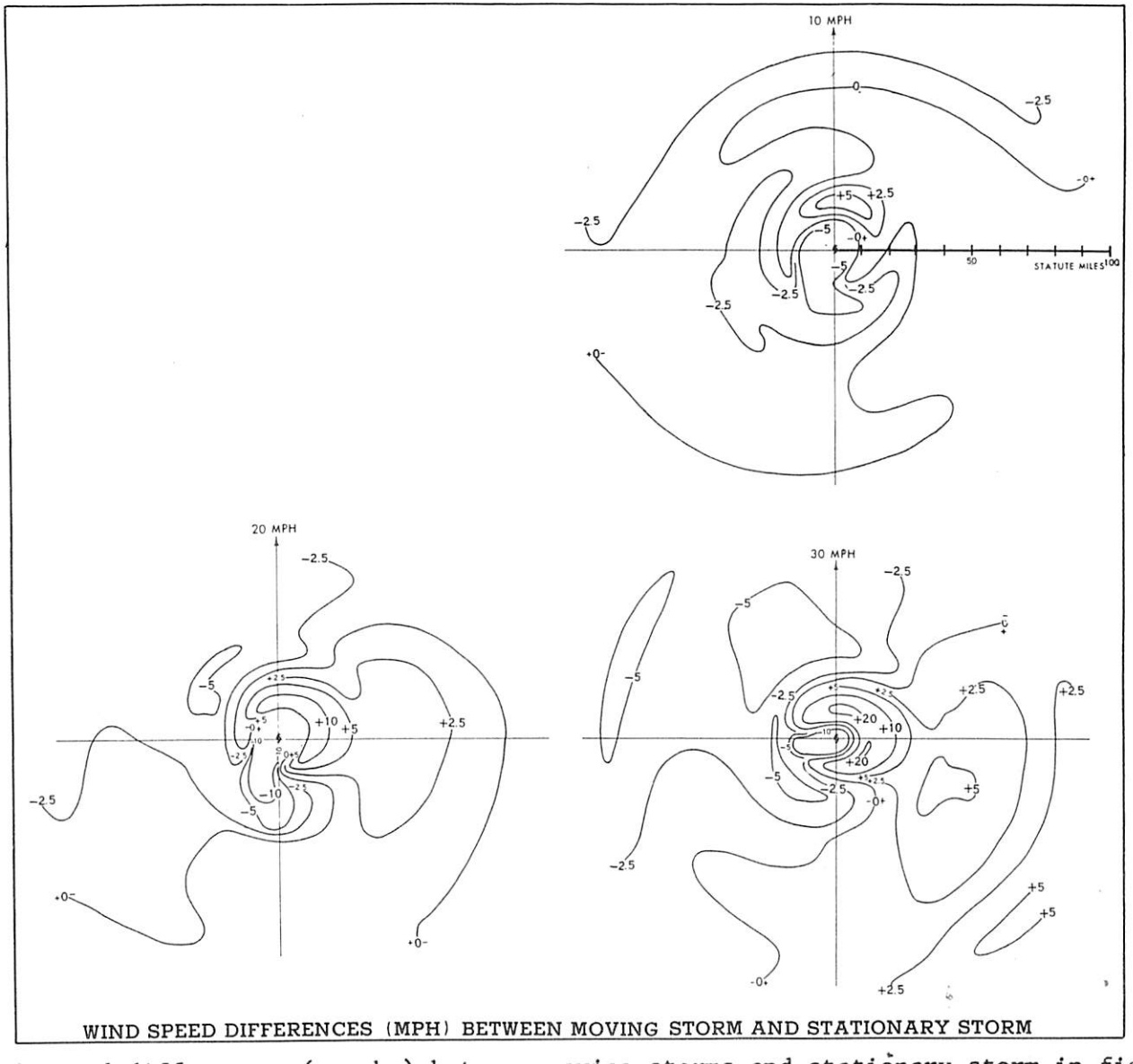

Figure 12. Wind speed differences (m.p.h.) between moving storms and stationary storm in figure 9.

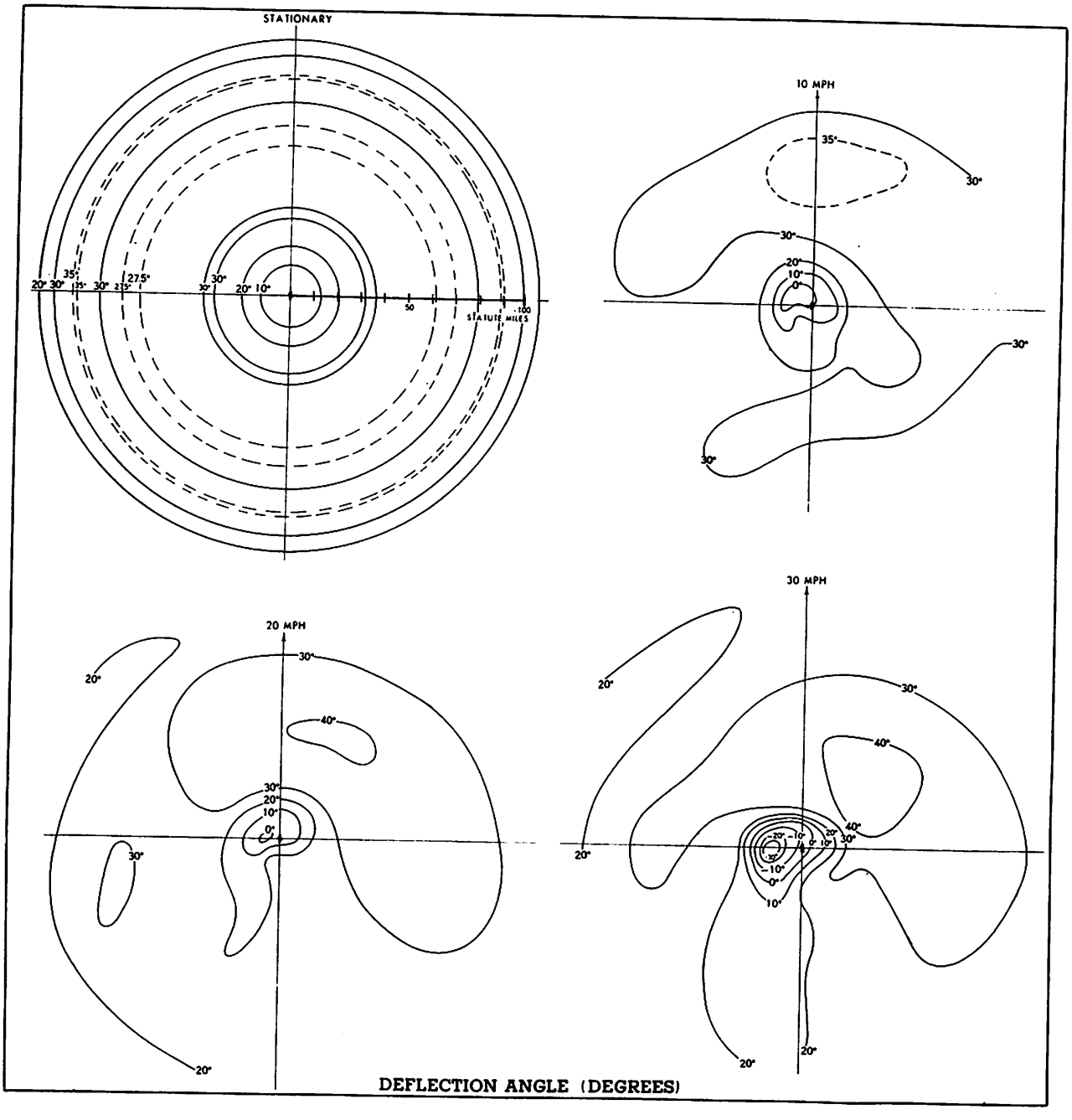

Figure 13. - Deflection angle fields in the stationary and moving storms. Same as figure 9.

The field of radial velocity components (fig. 10) shows an alignment of extreme value centers similar to the deflection angle centers of the corresponding 30 m.p.h. storm of figure 13. This consistent orientation supports what appears geometrically reasonable about the deflection angle making an important contribution to the radial component of the velocity in a moving storm.

7. EFFECTS OF AN INCREASE IN PRESSURE GRADIENT

Another important factor controlling hurricane surface winds is the pressure gradient. In view of the strong damping of the wind toward the local value of the equilibrium wind vector, it would be expected that the equilibrium wind equation would offer clues as to the differences in wind between storms of differing pressure gradient and also variations of the wind within one storm with an asymmetrical pressure field. Consider two circularly symmetrical stationary hurricane pressure fields, indicated by subscripts 1 and 2 respectively, such that at each radius,

$$\left(\frac{\partial p}{\partial r}\right)_2 = m\left(\frac{\partial p}{\partial r}\right)_1 \tag{30}$$

where m is constant, the same over-all radii. What are the corresponding ratios of V_{b_2} to V_{b_1} and β_{b_2} to β_{b_1}? Approximate ratios may be found from the respective equilibrium wind equations,

$$\frac{1}{\rho}\left(\frac{\partial p}{\partial r}\right)_1 \sin \beta_{b_1} - K_t V_{b_1}^2 = 0 \tag{31}$$

$$m\,\frac{1}{\rho}\left(\frac{\partial p}{\partial r}\right)_1 \sin \beta_{b_2} - K_t V_{b_2}^2 = 0 \tag{32}$$

$$\frac{1}{\rho}\left(\frac{\partial p}{\partial r}\right)_1 \cos \beta_{b_1} - fV_{b_1} - \frac{V_{b_1}^2}{r} \cos \beta_{b_1} - K_n V_{b_1}^2 = 0 \tag{33}$$

$$m\,\frac{1}{\rho}\left(\frac{\partial p}{\partial r}\right)_1 \cos \beta_{b_2} - fV_{b_2} - \frac{V_{b_2}^2}{r} \cos \beta_{b_2} - K_n V_{b_2}^2 = 0 \tag{34}$$

First, dividing (32) by (31) yields the joint relation

$$V_{b_2} = V_{b_1}\left(m\,\frac{\sin \beta_{b_2}}{\sin \beta_{b_1}}\right)^{\frac{1}{2}} \tag{35}$$

The equilibrium wind nomogram, figure 3, shows that as the pressure gradient is varied while r is held constant, β_b changes slowly in general in comparison with V_b. This suggests that the following particular solution of equations (31), (32), and (35) be tested as a solution of (33) and (34):

$$\beta_{b_1} = \beta_{b_2} \tag{36}$$

$$V_{b_2} = V_{b_1} m^{1/2} \tag{37}$$

Now inserting (37) in (34), and combining with (33), the concomitant relation of deflection angles is:

$$\cos \beta_2 = \left(\frac{m^{-1/2} fV_{b_1} + K_n V_{b_1}^2}{fV_{b_1} + K_n V_{b_1}^2} \right) \cos \beta_1. \tag{38}$$

Equations (36 and (37) are the desired approximate solutions of (31)-(34) to the extent that (38) is equivalent to (36). The value of the fraction in (38) is slightly less than 1 for m greater than unity. The departures will be illustrated by an example.

Let the subscript 1 apply to the basic pressure field of the model hurricane and let m = 1.4. At r = 50 mi.:

$$V_{b_1} = 55.5 \text{ m.p.h.}$$

$$V_{b_1}^2 = 3080 \text{ (m.p.h.)}^2$$

$$f = .238 \text{ hr.}^{-1} \quad (27°N)$$

$$K_n = .020 \text{ mi.}^{-1}$$

$$\beta_{b_1} = 28.8°$$

$$\cos \beta_{b_1} = .8763$$

With these values, the respective β_{b_2}'s from (36) and (38) are 30.7° and 28.8°, while the respective V_{b_2}'s from (37) and (35) are 65.5 m.p.h. and 64.2 m.p.h. Thus it is seen that (36) and (37) are good, but not excellent, approximate solutions of (31)-(34).

The inferences are that, in view of the close relation of the surface wind to the equilibrium wind, the square of the surface wind speed at a given radius in the more vigorous part of a hurricane, other things being equal, will be approximately proportional to the pressure gradient, while the deflection angle will not be greatly affected.

The inferred relation of wind speed to pressure gradient was tested by constructing trajectories. A 40 percent increase in the basic model pressure gradient was obtained by increasing $(p_n - p_o)$ of equation (1) by 40 percent. As before, trajectories were computed from a 120-mile radius in this intensified, but stationary, pressure field.

The resulting speed profiles may be compared with one profile based on the initial pressure field in figure 14. The oscillations of the speed profiles with unbalanced initial conditions were soon damped as before. The 40 percent increase in the pressure gradient produced a roughly 20 percent average increase in the speed. These results substantiate that for frictional flow in which the friction is proportional to the square of the wind speed, the square of the wind speed tends to be proportional to the pressure gradient. This result is consistent with the principle of the kinetic energy increase being equal to the net work done.

8. CORIOLIS PARAMETER AND ASYMMETRY OF THE WIND FIELD

At latitudes at which hurricanes are found the Coriolis parameter varies about 10 percent along a north-south line 200 miles long. The previous trajectories and the equations of horizontal motion permit the following deductions: Variation in the Coriolis parameter can account for but a small variation in the wind speed. Consider first the inner region of the hurricane. Here we have two other forces normal to the wind vector, the centrifugal force and the normal component of friction, either being nearly an order of magnitude larger than the Coriolis force. Secondly, more of the asymmetry induced by the Coriolis parameter will appear in the deflection angle than in the speed. This is because frictional damping has a more direct effect on the speed than on the direction. The wind speed asymmetry that can be ascribed to the Coriolis parameter is somewhat less than that in the upper right-hand panel of figure 11, ascribed to 10 m.p.h. forward motion of a symmetrical pressure field. The highest speeds and largest deflection angles from the Coriolis parameter asymmetry will tend to be downwind of the south side of the storm, regardless of direction of motion, but will tend to be masked by the larger storm-motion effects.

9. MODIFICATION OF WIND PROFILES BY ALTERATION OF FRICTIONAL COEFFICIENTS

The trajectories can also give information on whether the characteristics of the two-dimensional flow in the hurricane at anemometer level apply at other levels in the friction layer.

In a typical hurricane, outside the eye, the horizontal pressure gradient force changes little with height in the lowest several thousand feet.

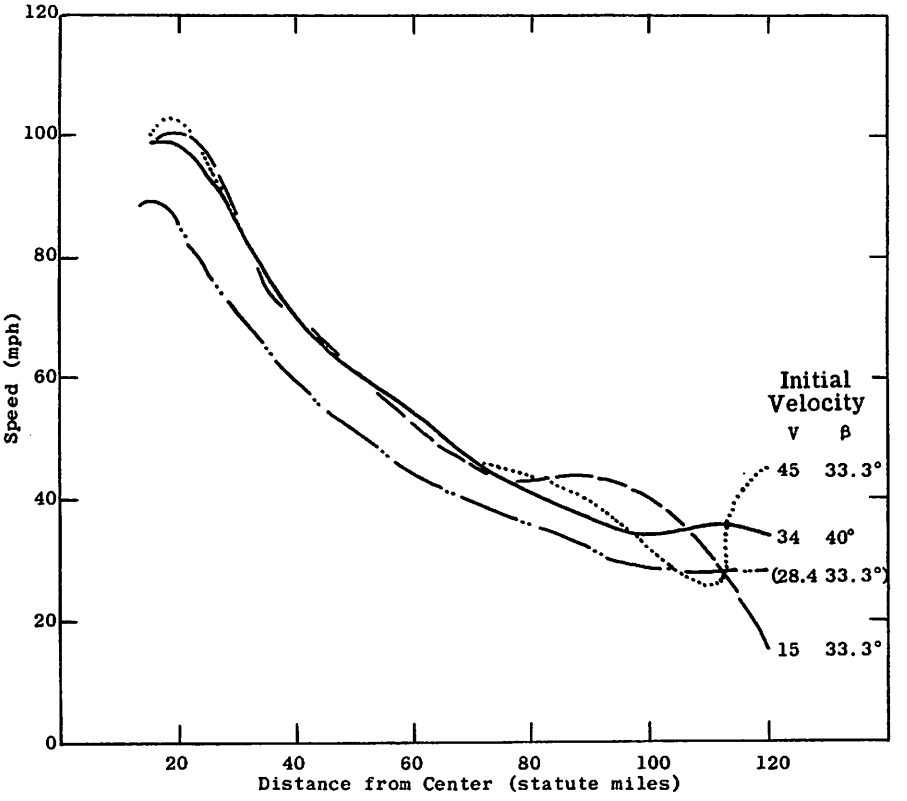

Figure 14. - Surface wind speeds in stationary hurricane. Pressure gradient increased 40 percent for three upper curves.

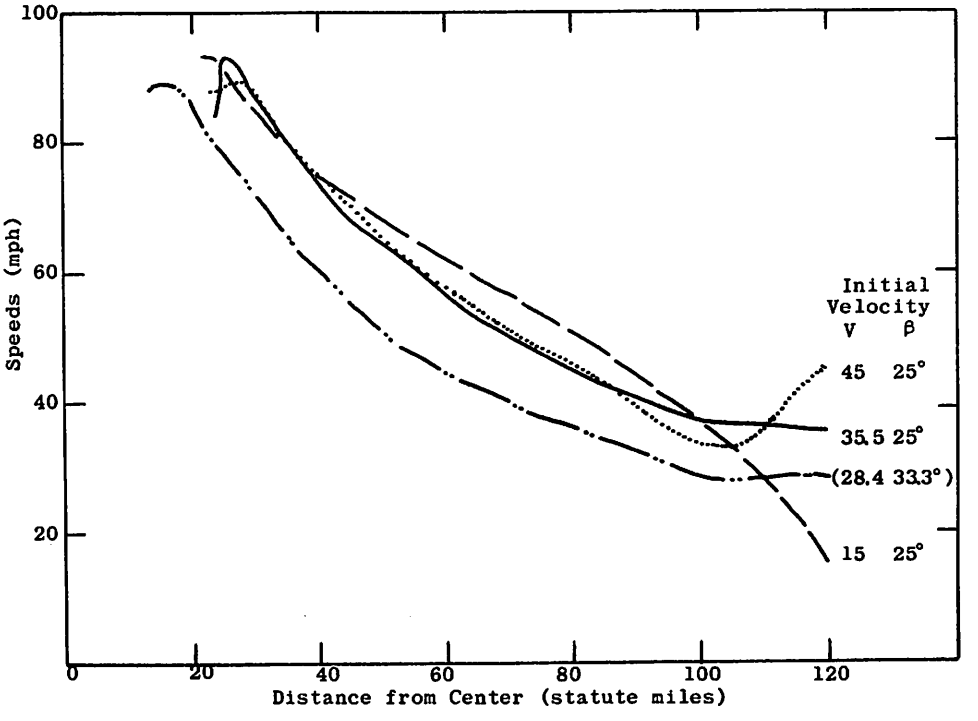

Figure 15. - Surface wind speeds in stationary hurricane. Friction coefficients reduced 50 percent for three upper curves.

The coefficients of friction, on the other hand, decrease rapidly with increasing distance from the underlying surface. Therefore flow at various levels may be simulated by computing trajectories as before through the same field of pressure gradient force, but with reduced values of friction.

Figure 15 shows the speed profiles for such trajectories computed with friction again having components both opposite and normal to the wind but with coefficients one-half their anemometer-level values. It is seen that profiles from speeds with differing initial velocities converge as before, but that the damping of the speed is slower, as would be expected with less friction. Comparative central damped values of speed and direction for the two differing frictional levels have been listed in table 4. At the upper level, the speeds are greater (20 percent to 30 percent) and the deflection angle smaller (out to r = 60 mi.) than at anemometer level, as would be expected. The tangential frictional acceleration ($K_t V^2$) is 10 percent to 30 percent less.

The general character of these results would not be altered if modest departures were permitted from two assumptions made, namely that the ratio of the tangential friction coefficient to the normal coefficient is constant with height, and that the frictional acceleration remains proportional to the square of the speed instead of to some different power of the speed.

It is seen that as the friction decreases upward the corresponding increases in speed are reasonable.

10. REGIONS AND ASPECTS OF CONVERGENCE

The horizontal forces controlling low-level hurricane winds have been considered up to this point. The hurricane winds are related in an equally fundamental way to interactions in the vertical. This section will present some speculations that attempt to relate the low-level horizontal wind field to the energy source. We might regard the heart of the hurricane as the region where the maximum low-level convergence occurs. That is probably where the most ascent takes place, where the most latent-heat is released, and is the "sink" which removes air from the lower levels. The horizontal convergence is readily computed from the trajectories that were constructed, and is found to be concentrated near the eye. Figure 16 (right panel) shows the convergence for the 20 m.p.h. hurricane for which other data are shown in figures 11, 12, and 13. The outer solid curves are obtained graphically from

$$\vec{\nabla}_2 \vec{V} = \frac{A_2 - A_1}{\frac{1}{2}(A_2 + A_1)(t_2 - t_1)}$$

where the A's refer to areas of a small polygon at successive times, t_1 and t_2. An average value of convergence near the center could be closely determined from the same formula, but with the polygon encompassing the entire central region of the hurricane. The exact distribution within the central

Table 4. - Comparison of wind with differing friction coefficients after approaching central damped value

	Anemometer-Level Friction $(K_t)_1 = .022$ mi.$^{-1}$			One-Half Anemometer Level Friction $(K_t)_2 = .011$ mi.$^{-1}$				
Radius (Statute Mi.)	Speed, V (mi.hr.$^{-1}$)	Deflection Angle, β (degrees)	$(K_t)_1 V^2$ (mi.hr.$^{-2}$)	Speed, V (mi.hr.$^{-1}$)	Deflection Angle, β (degrees)	$(K_t)_2 V^2$ (mi.hr.$^{-2}$)	Ratio of Speeds	Ratio of $K_t V^2$
80	36	28	28.5	47	35	24.3	1.30	.85
70	39	27	33.5	52	32	29.7	1.33	.89
60	44	29	42.6	59	29	38.3	1.34	.90
50	52	30	55.9	66	28	47.9	1.27	.86
40	60	30	79.2	74	23	60.2	1.24	.76
30	71	29	110.9	86	20	82.1	1.21	.74
25	78	27	133.8	91	15	92.0	1.17	.69

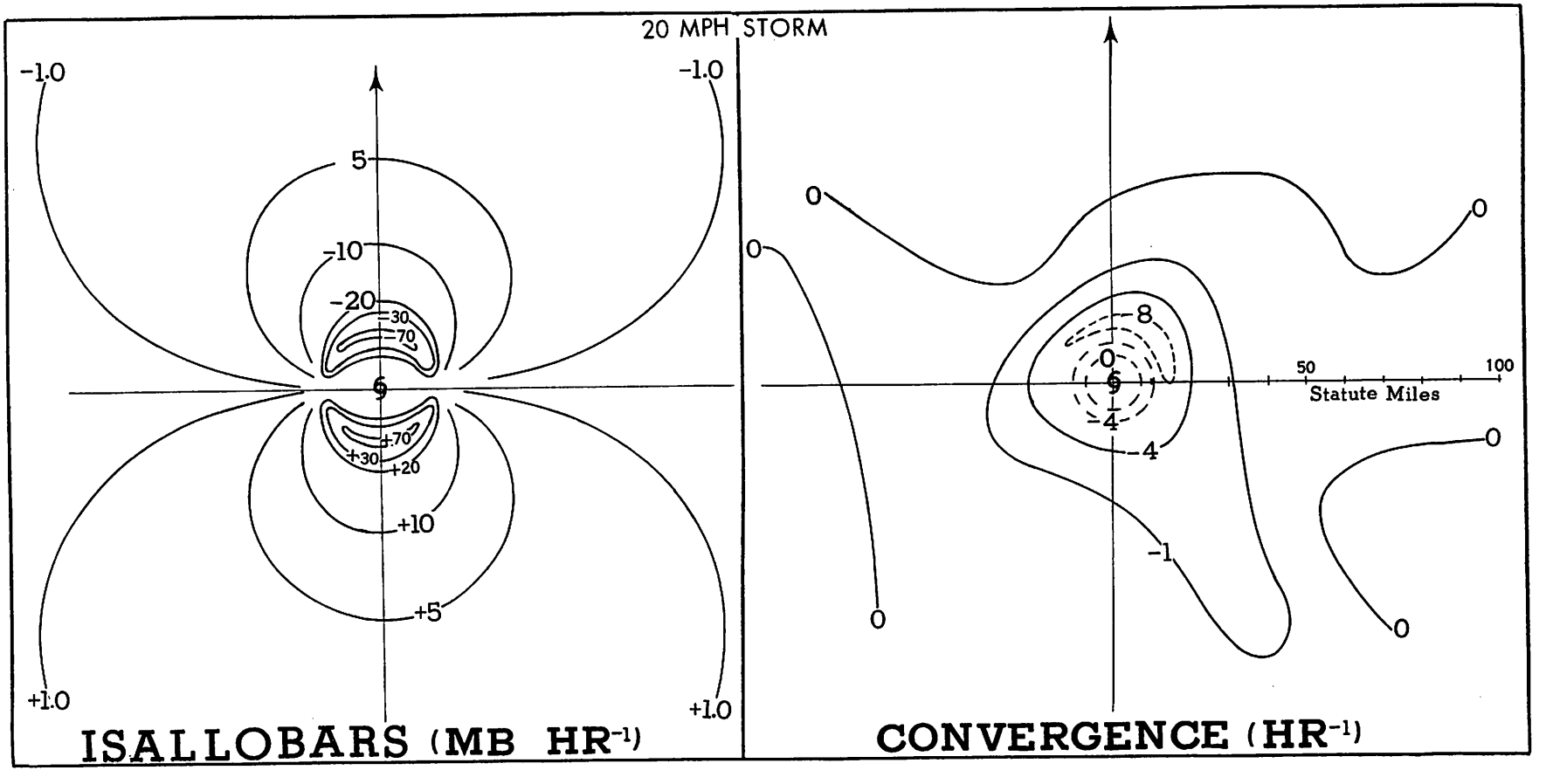

Figure 16. - Convergence and isallobaric fields for 20 m.p.h. hurricane of figure 9.

region is not obtained from the trajectories because they overlap, intersect, and become indeterminate. It can be assumed that the convergence is near zero over a substantial portion of the eye. The combination of necessary average values of convergence within the "4" isopleth of figure 16, right panel, together with the assumed zero area, can be obtained only by a tight band of high values around the circle corresponding roughly to the position of the eye wall. The "8" center ahead of the storm center is largely based on the preceding deduction.

The streak of higher convergence values to the right rear is associated with the asymptote of confluence between air entering the storm directly from the right and right-rear sides and the air curving into the storm after passing around the left side.

As an argument in favor of the largest convergence values being found in front of the storm, consider the isallobars shown in the left panel of figure 16*. Since both the isallobars and the region of maximum convergence are related to flow patterns at high levels that are favorable for divergence, and to warming and vigorous vertical motions in the region of maximum convection, it would be expected that the isallobaric center and the convergence center would be near each other. In a moving hurricane, the sea level isallobaric center must lie ahead of the storm center, except in rare circumstances. Therefore there is reason for seeking the convergence center in advance of the storm center.

As the center of maximum convergence moves, it must be fed by a current of low-level wind toward that place. If the maximum convergence is located as shown in figure 16, because of the circular nature of the hurricane this "feeding current" must come around the right side of the storm in a slow-moving hurricane. In a fast-moving hurricane the "feeding current" could come from the right-front quadrant. We speculate that the feeding current in the Tropics will tend to be drawn from the environmental air of the highest wet-bulb temperature and that mutual adjustments of the pressure field, the vertical motion field, and the horizontal velocity field will tend to produce the highest horizontal velocities in this current. The highest velocities will tend to be found most often somewhere on the right side of the moving storm in the Tropics but not at any geometrically predetermined radius or bearing, as small variations in air mass characteristics, and other non-geometric factors, exercise control. In hurricanes that are tapping an extra-tropical source of energy, the maximum winds might be expected in any quadrant, depending on many complicated factors.

---

*As an incidental item, we draw attention to the coincidence that the isallobaric pattern in the left panel of figure 16 is strikingly similar to the field obtained by Kasahara(/10/ his fig. 1(b)) representing the individual time rate of deformation of a moving vortex pattern, depending on the gradient of the absolute vorticity. The patterns are not only alike in shape, but are similarly antisymmetric.

11. ASPECTS OF ASYMMETRY IN HURRICANE WIND FIELDS

It has been accepted since the days of sailing vessels that the strongest winds and the largest area of gale speeds are most often found to the right of the path of a hurricane. Thus the term "dangerous semicircle" has come to be applied to the right half. One commonly accepted explanation is that the asymmetrical hurricane wind field is the necessary resultant of a combination of rotational and translational velocity. This theory has been promulgated by distinguished individuals. Ferrel [17] in his monumental Popular Treatise on the Winds wrote that "both in the middle and tropical latitudes the velocity of cyclonic motion is increased on the right-hand side of the path of the center, and decreased on the left-hand side, by the progressive motion of the air in the neighborhood of the cyclone... The right-hand side, therefore, in the Northern Hemisphere has long been recognized as the dangerous side of the cyclone... In endeavoring, therefore, to escape the most dangerous part of the cyclone, care should be taken to avoid if possible this side." Sir Napier Shaw [20] in debating the nature of extra-tropical cyclones with the Norwegian School noted, "the fact (which ought to have been obvious to anyone during the last fifty years) that if the revolving fluid were carried along by a current of air the winds would represent, not simply the rotation, but the combination of translation with rotation." Previously, Shaw (1919) clearly regarded cyclones as bodily advancing masses of rotating air. For a recent reference we quote from Morgan, et al. [13]: "In all cases the greatest force of wind and wave is concentrated in the right side of the circular storm." "This results from the additional wind speeds acquired by the forward motion of the storm." "The other semicircle--often called the 'safe' side--experiences the opposite effect; that is, the forward movement of the storm results in decreased wind speeds." Another recent source (U. S. Navy Hydrographic Office [23]) refers to "that part to the right of the storm track" as the dangerous semicircle because "the actual wind speed is greater than that due to the pressure gradient alone, since it is augmented by the forward motion of the storm."

Going back to an earlier time, however, it is interesting to note that Reid [16], who prepared the first sailors' rules for navigating in a hurricane, in referring to the right front quadrant as the quadrant of greatest danger (left front in Southern Hemisphere) implied no notion that the winds are stronger here than in other quadrants. He had in mind rather that a sailing vessel running before the wind in this quadrant encounters the grave risk of being carried around in front of the moving storm and being subjected to the extreme winds near the center as the storm progresses. The authors of the present report regard the common explanation of asymmetry given in the previous paragraph as fallacious and an impediment to understanding hurricanes, and even dangerous if applied indiscriminantly as a navigational rule. This section will set forth our viewpoint.

That the strongest winds are occasionally on the left side of a moving hurricane is shown by hurricane Carrie, the most severe hurricane of the 1957 season in the Atlantic. On September 21, 1957, the German schooner Pamir

capsized and was destroyed in the left side of the storm. Rodewald /17/ estimates from logs of other ships that, at the time of the sinking, wind forces in the left rear quadrant (frequently a relatively favorable quadrant) were two and one-half forces higher on the Beaufort scale than at corresponding positions in the right front quadrant (frequently a relatively unfavorable quadrant). Rodewald speculates that the ship's master may have sailed across the front of the advancing hurricane to the most severe part of the storm in an attempt to follow the rule to gain the "navigable" /left/ semicircle, which in this instance turned out to be the most dangerous one. This tactic, of course, was contrary to Reid's rule not to run before the wind in the right front quadrant.

For the sake of completeness, we point out that LaSeur /11/ in commenting on an analysis of the wind field at 500 mb. in the hurricane of September 17, 1955, said that "maximum speeds ahead of and behind the storm center are about the same, but wind speeds to the right of the center are significantly greater than those to the left. The difference of about 25 knots is essentially twice the speed of the storm. On the basis of this distribution of speeds one might consider the horizontal motion near the eye at this level to be composed primarily of a translation plus the rotation of the storm. However, the presence of large variable vertical motions complicates this simple picture."

The heart of the rotation-plus-translation fallacy is that a law of motion of solid bodies has been misapplied to a fluid. The parts of a solid body are firmly bound to each other by internal forces; each part must therefore respond to a torque applied to any part of the body, thus gaining a rotational component of velocity. A straight line force through the center of gravity of the body will impart a translational velocity to the entire body. In the hurricane, on the other hand, the shearing stresses between air particles horizontally adjacent are negligible; a torque is therefore impossible. The only real forces affecting the motion of each air particle are the 3-dimensional pressure gradient force, the vertical shearing stress, and gravity. Only the <u>local</u> magnitude of these forces affects the motion of the particle. One might say that the air has no knowledge of forces applied at other places and does not react to them.

The other aspect of the fallacy is the concept of a uniform basic current of parallel flow. Hypothesize a sink vortex imbedded in uniform parallel flow, and moving at the rate of the basic flow. Let the pressure gradient forces in the vortex be radially symmetrical about its center and neglect friction. This model would obviously produce a wind field which fits the rotation-plus-translation description. The component of velocity equal to the initial velocity of the basic current would be the translation component, while the component acquired from the radially symmetrical field of acceleration would be the rotational component. But there is a fundamental incongruity in this model! A sink vortex cannot be imbedded in uniform parallel flow. Continuity of mass is impossible. Tropical meteorologists would immediately call attention to the fact that singularity points must always occur in <u>pairs</u>. The complex fashion in which a hurricane vortex must blend with its envoronment is illustrated by Sherman /21/ in his figure 1.

In summary, the resolution of hurricane wind velocities into "rotational" and "translational" components, to be anything more than an exercise in geometry, requires either of two conditions--that the respective components be related to different kinds of forces within the hurricane, or that they be related in some differing fashion to the momentum of the air before it entered the hurricane. Neither is tenable. The rotation-plus-translation concept should not be applied to fluids.

The contributing factors to the asymmetry of the typical hurricane surface wind field can be identified from the fundamental equation of motion (2): (1) asymmetry of the Coriolis parameter, (2) asymmetry of friction coefficients, (3) asymmetry of velocity at the periphery of the storm, (4) motion of the pressure field, and (5) asymmetry of the pressure field. The relative significance of each factor may be assessed from the results given in this paper. First, the Coriolis parameter relates only to a north-to-south asymmetry rather than asymmetry from left to right with respect to the storm path, and furthermore, as discussed in section 8, it is small in comparison with other causes. Secondly, for a storm entirely over open sea it is difficult to envision a circumstance which would produce any significant asymmetry in the friction coefficients other than that produced by the wind itself by a differential roughening of the sea surface. Such a wind-dependent variation is part of the exponent and coefficient in equation (8). In a hurricane moving partly over land, the asymmetry of the friction coefficients becomes a major control on the character of the wind field. Thirdly, it was found in this study that, because of the frictional damping of the wind toward an equilibrium value, initial velocities have only a minor effect on subsequent velocities; that is, asymmetry of the peripheral velocity makes little contribution to the asymmetry of the wind in the heart of the storm.

Motion of the pressure field was found, by construction of dynamic trajectories in this study, to produce an appreciable but not large asymmetry of the hurricane wind field, considerably less than would be deduced from application of a rotation-plus-translation computation.

Thus it is deduced, by elimination of the other major factors, that the primary mechanical cause of the asymmetry of a hurricane surface wind field is an asymmetry of the pressure gradient field. This is consistent with the findings of the relation of wind to pressure gradient in this study. A significant secondary factor is the motion of the pressure field. All other factors are relatively inconsequential. The causes of pressure gradient asymmetry bear further investigation. Probable important factors are patterns of divergence aloft, asymmetry of moisture and temperature in the air mass surrounding the storm, and the necessity of a feeding current which enters the front of a fast-moving hurricane. Two examples of hurricanes with maximum winds in sectors other than the right semicircle are the hurricane of the Pamir disaster already referred to (Rodewald /17/), and the hurricane of March 1904 over Delaware Bay, in which the strongest winds were to the rear (Spuhler /22/).

12. SUMMARY AND CONCLUSIONS

A manual technique for constructing trajectories has been adapted to include the effects of normal and tangential frictional forces. The technique has been applied to the simulation of hurricane wind fields. These wind fields, upon analysis, were shown to possess characteristics and properties that were reasonable and consistent with features that have prevailed in observed storms.

The dynamic factors associated with the form of hurricane surface wind fields have been described. The effects of variations in the dynamic factors have been studied in wind fields synthesized by the trajectory method. It has been demonstrated or deduced that:

(a) the asymmetry of inward spiraling trajectories increases with the speed of the hurricane;

(b) the portion of the periphery from which trajectories will fail to spiral in toward the center increases with the speed of the hurricane;

(c) while the highest speeds are generally found in the dangerous (right) semicircle, the difference between the wind speeds at points equally distant to the right and left of the center is much less than twice the speed of the storm, when motion is the only factor producing the asymmetry;

(d) the commonly observed asymmetry of the field of surface wind speeds in a moving hurricane can be primarily attributed to the effects of asymmetry in the horizontal pressure gradient, and not to motion per se. For centrosymmetrical pressure fields, speeds in the friction layer, at equal storm radii, tend to vary as the square root of the pressure gradient;

(e) by contrast to the previous item, asymmetry in the field of deflection angle in a moving hurricane is ascribed mostly to the motion of the storm, with variations in pressure gradient having only a secondary effect;

(f) the largest inward values of deflection angle for a moving storm occur in the right front quadrant. The fields of deflection angle were typically more heterogeneous than the isotach fields, in consequence of the greater frictional damping control on speed rather than direction;

(g) when unbalanced velocities are imposed upon the pressure field in a stationary storm, damping by the frictional forces rapidly brings both speeds and deflection angles back to near equilibrium values;

(h) the concept of an "equilibrium wind" for frictional flow, analogous to the gradient wind for frictionless flow, was formulated. The local surface wind velocity was found to approach closely the value of the equilibrium wind at the same point.

ACKNOWLEDGMENTS

Kendall R. Peterson of the U. S. Weather Bureau, Hydrometeorological Section, contributed many valuable suggestions. Thanks are also due Mrs. Cora G. Ludwig, Miss Edna L. Grooms, Mrs. J. M. Hughes, and Mr. Keith D. Bell.

REFERENCES

1. Wm. Ferrel, A Popular Treatise on the Winds, John Wiley and Sons, New York, 1889, 307 pp.
2. C. L. Godske, et al., Dynamic Meteorology and Weather Forecasting, American Meteorological Society, Boston, 1957, 800 pp. (See especially pages 453-454.)
3. H. V. Goodyear, "A Graphical Method for Computing Horizontal Trajectories in the Atmosphere," Monthly Weather Review, vol. 87, No. 1, 1959, pp. 188-195.
4. G. J. Haltiner and F. L. Martin, Dynamical and Physical Meteorology, McGraw-Hill Book Co., Inc., New York, 1957, 470 pp.
5. B. Haurwitz, "On the Relation Between the Wind Field and Pressure Changes," Journal of Meteorology, vol. 3, No. 3, 1946, pp. 95-99.
6. B. Haurwitz, "Comments on the Sea-Breeze Circulation," Journal of Meteorology, vol. 4, No. 1, 1947, pp. 1-8 (see p. 2).
7. L. F. Hubert, "Distribution of Surface Friction in Hurricanes," Journal of Meteorology, vol. 16, No. 4, 1959, pp. 393-404.
8. L. A. Hughes, "On the Low Level Wind Structure of Tropical Storms," Journal of Meteorology vol. 9, No. 6, 1952, pp. 422-428.
9. Hydrometeorological Section, U. S. Weather Bureau, "Analysis of Winds Over Lake Okeechobee During Tropical Storm of August 26-27, 1949." Hydrometeorological Report No. 26, 1951, 80 pp.
10. A. Kasahara, "The Numerical Prediction of Hurricane Movement with the Barotropic Model," Journal of Meteorology, vol. 14, No. 5, 1957, pp. 386-402.
11. N. E. LaSeur, "An Analysis of Some Detailed Data Obtained by Aircraft Reconnaissance of a Hurricane," Scientific Report No. 5, on contract Florida State Univ. 1957, 25 pp.
12. W. Malkin, "Filling and Intensity Changes in Hurricanes Over Land," National Hurricane Research Project Report No. 34, 1959, 18 pp.
13. J. P. Morgan, et al, "Morphological Effects of Hurricane Audrey on the Louisiana Coast," Technical Report No. 10, Coastal Studies Institute, Louisiana State Univ., June 1, 1958, 53 pp.
14. V. A. Myers, "Characteristics of U. S. Hurricanes Pertinent to Levee Design for Lake Okeechobee, Florida," U. S. Weather Bureau, Hydrometeorological Report No. 32, 1954, 106 pp.

15. V. A. Myers, "Surface Friction in a Hurricane," Monthly Weather Review, vol. 87, No. 8, 1959, pp. 307-311.
16. W. Reid, The Law of Storms, London, 1850.
17. M. Rodewald, "Hurricane Carrie and the Pamir Disaster," Weather, vol. 13, 1958, pp. 337-349.
18. R. W. Schloemer, "Analysis and Synthesis of Hurricane Wind Patterns over Lake Okeechobee, Florida," U. S. Weather Bureau, Hydrometeorological Report No. 31, 1954, 49 pp.
19. W. N. Shaw, Manual of Meteorology, Vol. IV. Cambridge University Press, 1931, 342 pp.
20. W. N. Shaw, "The Birth and Death of Cyclones," (lecture on July 22, 1920), Geophysical Memoirs No. 19, Meteorological Office Air Ministry, London, 1922, p. 214.
21. L. Sherman, "On the Wind Asymmetry of Hurricanes," Journal of Meteorology vol. 13, No. 5, 1956, pp. 500-502.
22. W. S. Spuhler, "Intensification of a Tropical Storm at High Latitude," Monthly Weather Review, vol. 85, No. 8, 1957, pp. 273-278.
23. U. S. Navy Hydrographic Office, American Practical Navigator. H. O. Publication No. 9, 1958, 1524 pp., (see especially p. 828).

APPENDIX

Manual Construction of Trajectories by the "Arc-Strike" Technique

Many and various schemes have been devised for manually computing dynamic trajectories. The unique features of the technique to be described are:

a. the inclusion of both tangential and normal frictional components.

b. the use of nomograms to avoid the actual construction of the very large geostrophic wind vectors that are characteristic of hurricane pressure fields.

1. Plot the wind displacement vector, $\vec{V}_1\Delta t_1$, with origin at a given distance and azimuth from the storm center ($\vec{AC}$, fig. 17). The sense of the initial vector is determined by the known or given deflection angle. The magnitude of the time increment, Δt, is decreased as the trajectory approaches the center, from 1/2 hour down to 3 minutes, by steps, as indicated in figure 18. The selection of a magnitude for the time increment, Δt, involves a compromise between the use of large time increments whereby accuracy and detail are sacrificed for ease and rapidity in performing the manual labor, as against shorter time intervals which give more refinement (up to a limiting point) but require tedious and painstaking manipulations with the drawing instruments.

2. Find the mid-point, M, of $\vec{V}_1\Delta t_1$ $(\vec{AC})$.

3. Draw the line HMP, with $\vec{AP}$ perpendicular to HMP. Point H is located in the direction of motion from the storm center at a distance given by $\left(\frac{\text{speed of storm}}{2}\right)(\Delta t)$. Note that when the storm is stationary, point H remains at the storm center.

4. Measure the distance HM. Then get the geostrophic speed $\left|\vec{V}_{g1}\right|$, corresponding to the given pressure field at a distance HM from the center.

5. Compute $\left|\vec{V}_{g1}\right|\Delta t_1$, as the magnitude of the vector from A, perpendicular to HM, the end point being marked B in the figure. Draw $\vec{BC}$, which represents the ageostrophic displacement, by definition.

ALTERNATE TO STEPS 5 AND 6. When using a reasonable working scale, such as 10 statute miles to the inch, point B may nevertheless extend some 2 feet or more from point A. One may circumvent running off the paper when

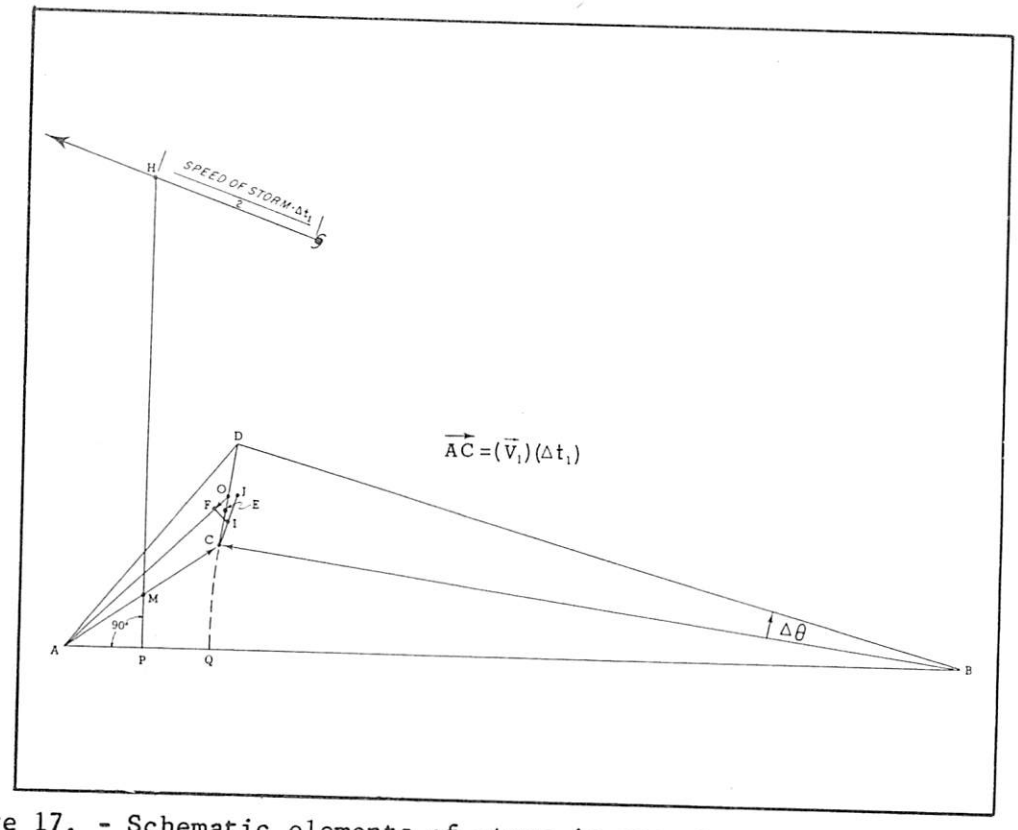

Figure 17. - Schematic elements of steps in manual construction of trajectories.

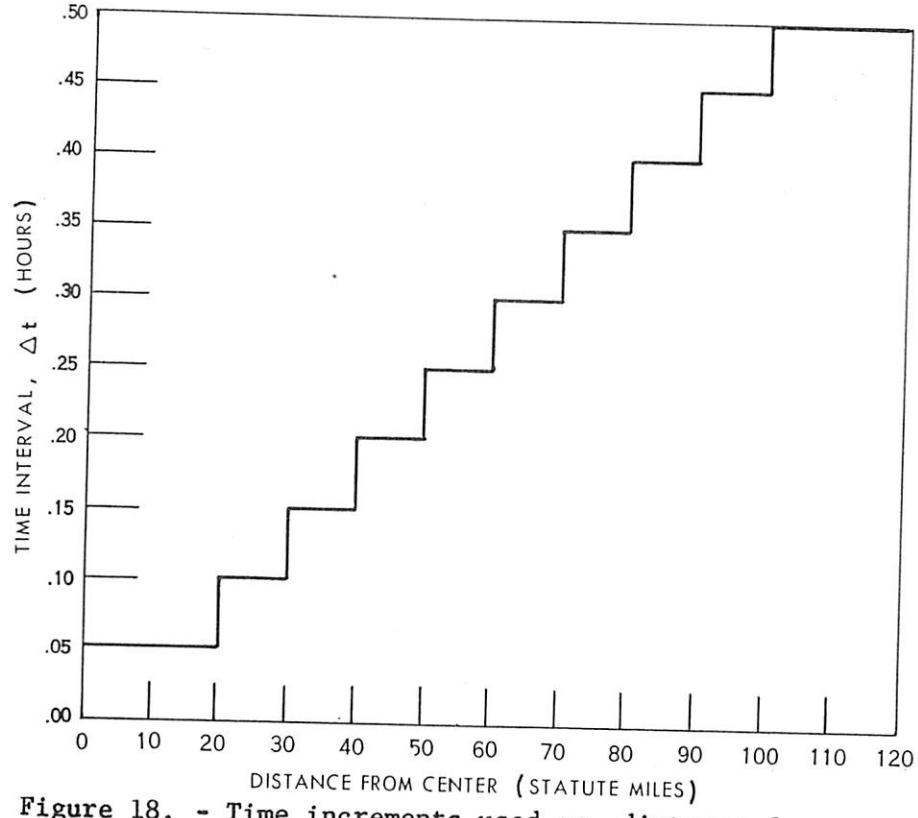

Figure 18. - Time increments used vs. distance from center.

drawing line AB, and omit drawing lines BC and BD, by a scheme that makes use of the nomograms Y and Z of figures 19 and 20 respectively. The scale of nomogram Y must be the same as the scale of the map on which the trajectories are constructed. The centers of the arcs lie on the baseline, at the indicated distances from 0. The base of nomogram Y is made to coincide with the segment AP, while simultaneously making point C lie on an arc of value $\left| \vec{V}_{g1}\Delta_1 \right|$. Determine the baseline distance on the nomogram corresponding to AQ.

Subtract the distance AQ from $\left| (\vec{V}_{g1}\Delta t_1) \right|$ to get $\vec{BC}$. Go into nomogram Z with the distance BC and the "arc-strike" angle $\Delta\theta$, as computed in step 6 below, to obtain the chord length CD. Use nomogram Y for the second time, lining up the base line along AB as before, with the origin at point Q. Then CD is drawn, such that point D falls on the arc through C.

---

6. Now swing an arc to the right around the point B, of radius BC, the magnitude of the angle or "arc strike" being determined by: $\Delta\theta = \Delta t\ f$, following Goodyear (1959), where:

f is the Coriolis parameter
Δt is the time increment
$\Delta\theta$ is the angle, or "arc strike"

7. Draw $\vec{AD}$, which represents the wind displacement vector corresponding to the velocity at the end of the time increment, but with no friction.

8. Measure one-third of the distance CD, to point E. Experience has indicated that the line segment AE is an excellent approximation to the average speed in the interval <u>with</u> friction, and is therefore used as a necessary first approximation. This pseudo-displacement $\vec{AE}$, when divided by Δt, gives the best estimate of the velocity, $\vec{V}$, to be used in the next step.

9. Compute the tangential and normal frictional displacements. According to Myers (1959), the tangential frictional acceleration, is approximated by $.022\ V^2$, the normal acceleration, by $0.20\ V^2$. The corresponding displacements due to friction are obtained by applying the formula:

$$\text{displacement} = 1/2\ (\text{acceleration})\ (\Delta t)^2$$

using $\vec{F}_t$ and $\vec{F}_n$ for the respective accelerations.

10. Bisect CD at 0. $\vec{AO}$ is the average wind displacement without friction during Δt.

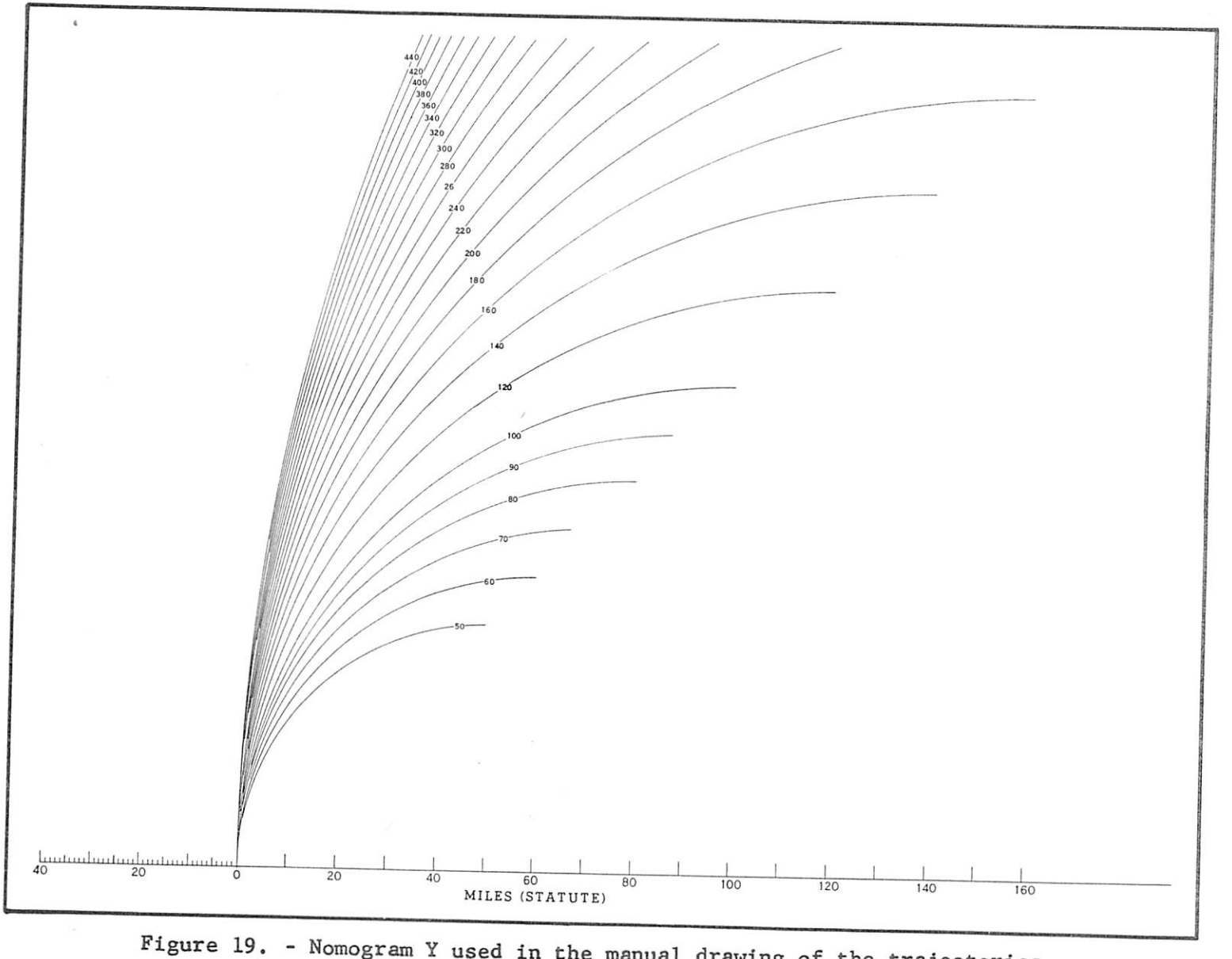

Figure 19. - Nomogram Y used in the manual drawing of the trajectories.

11. Plot the tangential frictional displacement $\vec{F}_t$ from 0 backward along $\vec{OA}$ to F, and plot F_n perpendicular to AO and to the right, from F to I. AI is the final average wind displacement with friction.

12. Extend CI to J, making CI = IJ. $\vec{AJ}$ is the final wind velocity displacement, representing the equivalent of $\vec{V}_2$ times Δt_1, shown in figure 1.

13. Repeat the process for the next step starting at I, but with initial speed equal to $\left| \vec{AJ} \right|$, and sense as given by $\vec{AJ}$.

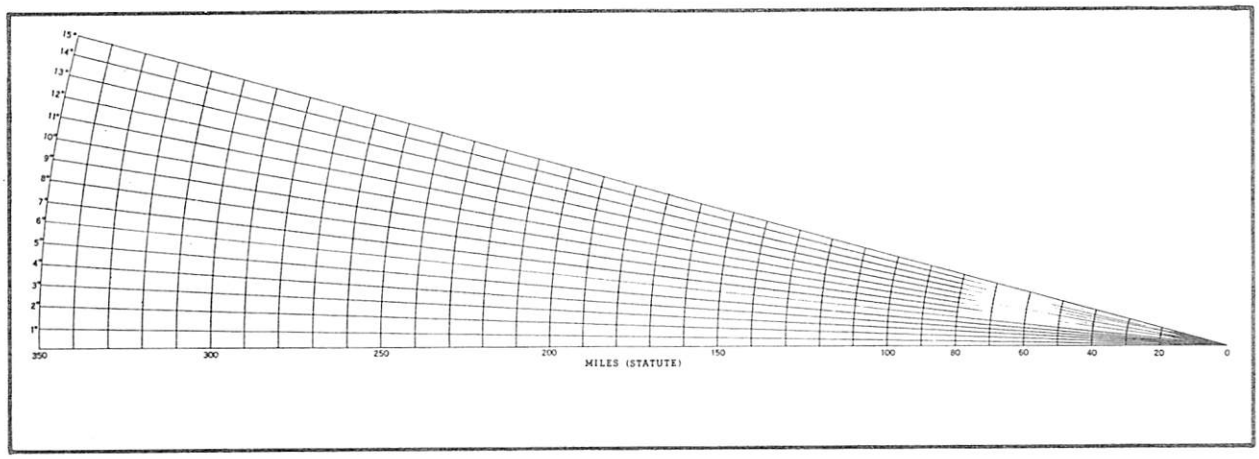

Figure 20. - Nomogram Z used in the manual drawing of the trajectories.